Magnetization dynamics, rheology, and an effective description of ferromagnetic units in dilute suspension

Patrick Ilg[1,*] and Martin Kröger[1,2,3]
[1]*Institut für Theoretische Physik, Technische Universität Berlin, Hardenbergstraße 36, D-10623 Berlin, Germany*
[2]*Institute for Theoretical Physics, University of California Santa Barbara, California 93106-4030*
[3]*Polymer Physics, Materials Sciences, ETH Zürich, CH-8092 Zürich, Switzerland*
(Received 27 April 2002; published 9 August 2002)

The rheological properties of a dilute suspension of ellipsoidal ferromagnetic particles in the presence of a magnetic field are studied on the basis of a kinetic model, where the flow and magnetic external fields couple in qualitatively different ways to the orientational behavior of the suspension. In the uniaxial phase the stress tensor is found to be of the same form as in the Ericksen-Leslie theory for nematic liquid crystals in the steady state. Expressions for a complete set of viscosity coefficients in terms of orientational order parameters are worked out. In the low Péclet number regime, the viscosity coefficients are given as explicit functions of the magnetic field and a particle shape factor, where the shape factor may equally represent a nonspherical unit (agglomerate, chain) composed of spherical particles. Effects due to possible flow-induced breakup of units are not covered in this work. Further, by considering the magnetization as the only relevant variable, a magnetization equation within an effective field approach is derived from the kinetic equation and compared to existing magnetization equations. The alignment angle of the magnetization and the first and second normal stress coefficient are studied for the special case of plane Couette flow. The assumptions employed are tested against a Brownian dynamics simulation of the full kinetic model, and a few comparisons with experimental data are made.

DOI: 10.1103/PhysRevE.66.021501 PACS number(s): 47.65.+a, 75.50.Mm, 83.80.Hj, 05.20.Dd

I. INTRODUCTION

Ferrofluids are colloidal suspensions of nanosized ferromagnetic particles in a carrier liquid [1]. Various technical applications use the fact that the rheological behavior of ferrofluids can be manipulated by external magnetic fields. While the rheological behavior of dilute ferrofluids is rather well understood, most commercial ferrofluids are more concentrated and show deviations from the behavior in the dilute regime [2,3]. In particular, the kinetic model of internal rotations of noninteracting, spherical ferromagnetic particles introduced in Ref. [4] successfully describes the rotational viscosity of dilute ferrofluids but is unable to account for various flow phenomena in commercial ferrofluids, such as a dependence on the symmetric velocity gradient, shear thinning, and the occurrence of normal stresses (see, e.g., [2] and references therein).

Recent years have seen intensive experimental [3,5,6] investigations of rheological properties of semidilute (commercial) ferrofluids subjected to an external magnetic field. Theoretical approaches to the dynamics of ferrofluids based on thermodynamic considerations have been proposed in Refs. [7–10]. Very recently, one coefficient appearing in the generalized magnetization equation proposed in Ref. [10] has been determined experimentally [11].

Extensions of the kinetic model [4] to dilute suspensions of ellipsoidal ferromagnetic particles have been proposed in Refs. [12–14]. Theoretical studies [12,13] investigate the initial part of the flow curve while Brownian dynamics simulations are performed in Ref. [14]. Nevertheless, until five years ago, ''The peculiarities of a rheological behavior of a suspension of ellipsoidal ferromagnetic particles in a field are scantily explored,'' p. 281 of Ref. [1]. Very recently, the kinetic model of ellipsoidal ferromagnetic particles was extended in Refs. [15,16] to include also polydispersity effects.

In the present work, we consider a Fokker-Planck equation approach [17] applied to the orientational dynamics of a suspension of rigid, noninteracting, ferromagnetic ellipsoidal objects whose magnetization is parallel to the bodies symmetry axis, and work out its explicit relation to the Ericksen-Leslie theory of nematic liquid crystals [18]. Five independent viscosity coefficients describe the magnetorheological homogeneous fluid. Their dependence on the orientational order parameters, the shape and concentration of the ferromagnetic units, and the solvent viscosity is worked out in detail. The Miesowicz viscosities, tumbling parameter, normal stress differences, and, e.g., the rotational viscosity increase, are related to combinations of these viscosity coefficients. In case of low Péclet number, explicit expressions for the coefficients, in terms of the magnetic field (in favor of the order parameters) are given and compared to previous results. Rheological properties due to possible flow-induced breakup of units are not covered in this work, but should be approximately obtained by superposition of the stated results for a given, yet unspecified, transient distribution. This work generalizes earlier results on the Fokker-Planck equation specialized to spherical ferromagnetic particles [19], where the effect of flow alignment of particle axes is not present. While uniaxial symmetry was the only assumption made so far, we use the stronger assumptions of the effective field approximation in order to derive a closed magnetization equation from the Fokker-Planck approach and discuss its relation to previous results. We also interpret the experimental result obtained in Ref. [11] for the tumbling parameter within the present kinetic model, and thereby conclude on

*Corresponding author. Email address: ilg@physik.tu-berlin.de

the nonspherical shape of ellipsoidal ferromagnetic units present in the sample. The validity of the presumption of uniaxial orientational symmetry made in the first part of this manuscript is finally tested against results obtained from a Brownian dynamics simulation of the full kinetic model in plane Couette flow. It is found that all viscosity coefficients are in good agreement with the results of the uniaxial approximation. The agreement is enhanced for strong magnetic field, resp. low Mason numbers. We stress that this agreement does not imply the actual distribution function to be almost uniaxially symmetric. Indeed, even for a large class of biaxial orientational distributions the moments that are relevant for the stress tensor are still rather well approximated by the uniaxial expressions. This finding actually motivated our analytical treatment of the uniaxial phase to be presented in Sec. III.

This paper is organized as follows: In Sec. II, the kinetic model of internal rotations of rigid, ferromagnetic, ellipsoidal units is introduced and some of its properties are discussed. The relationship between the kinetic model and the Ericksen-Leslie theory (summarized in Appendix A) is established in Sec. III. Comparison of the present approach to the results of Ref. [10] is made in Sec. IV as well as an interpretation of the experimental results obtained in Ref. [11]. For the special case of plane Couette flow, the alignment angle of the magnetization and the first and second normal stress coefficients are studied in Sec. III C. Finally, some conclusions are offered in Sec. VI.

II. KINETIC MODEL

Consider an ensemble of n noninteracting, identical, rigid, ferromagnetic ellipsoids per volume. We assume the system to be spatially homogeneous, so that the state is described by the probability distribution function $f(\boldsymbol{u};t)$ of an ellipsoid being oriented in the direction of the unit vector $\boldsymbol{u}$ at time t. Furthermore, it is assumed that the symmetry axis coincides with the direction of the magnetization of the particles, $\boldsymbol{\mu}=\mu\boldsymbol{u}$. The motion of a single ellipsoid is influenced by rotational diffusion, motion due to an external potential V, and the hydrodynamic drag caused by velocity field $\boldsymbol{v}$. The dynamics is conveniently described by the kinetic equation [1,17,20]

$$\tau\partial_t f=-\mathrm{Pé}\boldsymbol{\mathcal{L}}\cdot[(\tilde{\boldsymbol{\Omega}}+B\boldsymbol{u}\times\tilde{\boldsymbol{D}}\cdot\boldsymbol{u})f]+\frac{1}{2}\boldsymbol{\mathcal{L}}\cdot f\boldsymbol{\mathcal{L}}[\ln f+V/k_{\mathrm{B}}T], \tag{1}$$

where the potential V for a magnetic moment $\boldsymbol{\mu}=\mu\boldsymbol{u}$ in the local magnetic field $\boldsymbol{H}$ is given by

$$\frac{-V}{k_{\mathrm{B}}T}=\frac{\mu}{k_{\mathrm{B}}T}\boldsymbol{H}\cdot\boldsymbol{u}=h\hat{\boldsymbol{h}}\cdot\boldsymbol{u}=\boldsymbol{h}\cdot\boldsymbol{u}. \tag{2}$$

Here, the dimensionless magnetic field $\boldsymbol{h}=\mu\boldsymbol{H}/k_{\mathrm{B}}T$, its amplitude h (Langevin parameter), and the unit vector $\hat{\boldsymbol{h}}$ pointing in the field direction are introduced. In Eq. (1), $\boldsymbol{\mathcal{L}}=\boldsymbol{u}\times\boldsymbol{\nabla}_{\boldsymbol{u}}$ is the rotational operator with $\boldsymbol{\nabla}_{\boldsymbol{u}}$ being the gradient on the unit sphere. The dimensionless quantities $\tilde{\boldsymbol{D}}$ and $\tilde{\boldsymbol{\Omega}}$ characterize the flow geometry. The symmetric part of the flow gradient tensor and the vorticity are related to these quantities by $\boldsymbol{D}\equiv(\boldsymbol{\nabla v}+[\boldsymbol{\nabla v}]^T)/2=\|\boldsymbol{\nabla v}\|\tilde{\boldsymbol{D}}$, and $\boldsymbol{\Omega}\equiv(\boldsymbol{\nabla}\times\boldsymbol{v})/2=\|\boldsymbol{\nabla v}\|\tilde{\boldsymbol{\Omega}}$, respectively, where $\|\boldsymbol{\nabla v}\|$ denotes the norm of the velocity gradient, such that $\|\boldsymbol{\nabla v}\|=\dot{\gamma}$ for a shear flow with shear rate $\dot{\gamma}$. In Eq. (1), the Péclet number is introduced, $\mathrm{Pé}=\tau\|\boldsymbol{\nabla v}\|$, which measures the relative importance of viscous and Brownian forces on the particle orientation.

In order to interpret the results in terms of measurable quantities, we explicitly consider Eq. (1) to hold for ellipsoidal ferromagnetic units with positive axis ratio $r=a/b$, where each unit is composed of N ferromagnetic spherical particles (molecular substituents of the unit). Accordingly, r is restricted by N through $N^{-1/2}\leqslant r\leqslant N$, and $r=1$ and $r=N$ correspond to spherical and cylindrical units, respectively. In Eq. (1), $B\equiv(r^2-1)/(r^2+1)$, and $N=1$ implies $r=1$. Spherical units correspond to $B=0$. In that case, Eq. (1) reduces to the kinetic equation for dilute ferrofluids given in Refs. [1,4]. The relaxation time τ depends on the number of substituents N and axis ratio r via

$$\tau=e_r N\tau_1, \tag{3}$$

where $\tau_1\equiv\tau(N=1)=3\eta_s v_1/k_{\mathrm{B}}T$ is the relaxation time for an individual sphere with volume v_1 suspended in a Newtonian solvent with viscosity η_s. The dimensionless shape coefficient $e_r>0$ as a function of r is given in Appendix B. One has $e_1=1$ for spherical units and should use, e.g., e_N to describe cylindrical units. Using the above notation, number densities and volumes are related by $n=n_1/N$, $v=Nv_1$, however, concentration $\phi=nv$ and the products $n\mu$, nh to appear in the stress tensor remain unaffected by attaching a subscript 1 to all quantities. The relaxation time τ of the ellipsoidal unit is related to its rotary diffusion coefficient D_r and its rotary friction coefficient ζ_{rot} (see also Appendix B) via $D_r^{-1}=2\tau=\zeta_{\mathrm{rot}}/k_{\mathrm{B}}T$. Since the ellipsoidal unit is considered as agglomeration of individual spherical particles [15] each with magnetic moment μ_1, the magnetic moment of the ellipsoid is $\mu=N\mu_1$, i.e., $h=Nh_1$. The Mason number $\mathrm{Mn}\equiv\mathrm{Pé}/h$, to be used below, is related to the corresponding Mason number Mn_1 for a fluid of individual spherical particles by $\mathrm{Mn}=e_r\mathrm{Mn}_1$.

The hydrodynamic stress tensor $\boldsymbol{T}$ for an incompressible dilute suspension of rigid ellipsoidal particles can be decomposed into its symmetric and antisymmetric part, see Eq. (A4). The antisymmetric part reads

$$\boldsymbol{T}^{\mathrm{a}}=\frac{n}{2}\boldsymbol{\epsilon}\cdot\langle\boldsymbol{\mathcal{L}}V\rangle, \tag{4}$$

with the conventional total antisymmetric (Levi-Civita) tensor $\boldsymbol{\epsilon}$ of rank 3. Here and below, we use the following notation for averages of arbitrary functions $A(\boldsymbol{u})$ with respect to the distribution function f:

$$\langle A\rangle\equiv\int_{S_2}d^2uA(\boldsymbol{u})f(\boldsymbol{u};t), \tag{5}$$

where the integration is performed over the three-dimensional unit sphere. For convenience of notation the ex-

plicit dependence of f on time is frequently suppressed in the sequel. The symmetric part of the stress tensor reads, according to [1,20,21],

$$\boldsymbol{T}^{\mathrm{s}}=2\,\eta_{\mathrm{s}}(1+5\,\phi Q_1)\boldsymbol{D}+5\,\eta_{\mathrm{s}}\phi\{(2Q_3-BQ_0)(\boldsymbol{D}\cdot\langle\boldsymbol{uu}\rangle + \langle\boldsymbol{uu}\rangle\cdot\boldsymbol{D})-(Q_{23}-2BQ_0)\boldsymbol{D}:\langle\boldsymbol{uuuu}\rangle\}+\boldsymbol{T}^{\mathrm{pot}}, \tag{6}$$

where η_{s} is the shear viscosity of the Newtonian solvent. The geometric coefficients Q_i are defined in Appendix C and the potential contribution is given by

$$\boldsymbol{T}^{\mathrm{pot}}=\frac{nk_{\mathrm{B}}T}{2}B\langle[\boldsymbol{u}\boldsymbol{\nabla}\boldsymbol{u}+(\boldsymbol{\nabla}\boldsymbol{u}\boldsymbol{u})^{T}](\ln f+V/k_{\mathrm{B}}T)\rangle. \tag{7}$$

Inserting the potential (2) into Eq. (4) one obtains

$$\boldsymbol{T}^{\mathrm{a}}=\frac{nk_{\mathrm{B}}T}{2}(\boldsymbol{h}\langle\boldsymbol{u}\rangle-\langle\boldsymbol{u}\rangle\boldsymbol{h}). \tag{8}$$

Similarly, inserting the potential (2) into the potential contribution to the symmetric stress tensor, Eq. (7), gives

$$\boldsymbol{T}^{\mathrm{pot}}=\frac{nk_{\mathrm{B}}T}{2}B[6\langle\overline{\boldsymbol{uu}}\rangle-(\langle\boldsymbol{u}\rangle\boldsymbol{h}+\boldsymbol{h}\langle\boldsymbol{u}\rangle)+2\langle\boldsymbol{uuu}\rangle\cdot\boldsymbol{h}]. \tag{9}$$

where $\overline{\boldsymbol{uu}}\equiv\boldsymbol{uu}-(1/3)\mathbf{1}$ denotes the (symmetric) traceless part of $\boldsymbol{uu}$.

A. Equilibrium and stationary state

Stationary solution to Eq. (1) in the absence of flow are of the canonical form $f_{\mathrm{eq}}\propto\exp(-V/k_{\mathrm{B}}T)$. For the potential (2), f_{eq} takes the form

$$f_{\mathrm{eq}}(\boldsymbol{u})=\frac{h}{4\pi\sinh(h)}\exp(\boldsymbol{h}\cdot\boldsymbol{u}), \tag{10}$$

with the Langevin parameter h. Equilibrium moments $\langle A\rangle_{\mathrm{eq}}$ are defined by Eq. (5) with f replaced by f_{eq}. The equilibrium magnetization is $\boldsymbol{M}_{\mathrm{eq}}=n\mu\langle\boldsymbol{u}\rangle_{\mathrm{eq}}=n\mu L(h)\hat{\boldsymbol{h}}$, where $L(x)=\coth(x)-1/x$ is the Langevin function and $\hat{\boldsymbol{h}}=\boldsymbol{h}/h$ is the unit vector parallel to the magnetic field. This equilibrium magnetization is the classical result for a system of noninteracting magnetic dipoles.

For later use, we provide the magnetic susceptibility in equilibrium, which is given by $\chi_{\alpha\beta}=nk_{\mathrm{B}}T\chi_0\delta_{\alpha\beta}$ with $\chi_0=n\mu^2/(3k_{\mathrm{B}}T)$.

The stationary solution to Eq. (1) in case of steady potential flow, $\boldsymbol{\Omega}\equiv\mathbf{0}$, can also be found explicitly,

$$f_{\mathrm{s}}(\boldsymbol{u})=\frac{1}{z}\exp(\boldsymbol{h}\cdot\boldsymbol{u}+\mathrm{P\acute{e}}B\tilde{\boldsymbol{D}}:\boldsymbol{uu}), \tag{11}$$

where z is a normalization factor. One may define the Mason number Mn as $\mathrm{Mn}=\mathrm{P\acute{e}}/h$, which measures the relative importance of viscous and magnetic forces. For $B\mathrm{Mn}\ll1$, $f_{\mathrm{s}}\approx f_{\mathrm{eq}}$, while for $B\mathrm{Mn}\gg1$, f_{s} is independent of the magnetic field and determined completely by the flow. Accordingly, $f_{\mathrm{s}}=f_{\mathrm{eq}}$ holds strictly for spherical particles and also in equilibrium ($\mathrm{P\acute{e}}=0$).

B. Approach to equilibrium

In the absence of a flow field, Eq. (1) yields a unique equilibrium state f_{eq}. The approach to equilibrium is monitored by the dimensionless free energy functional per particle,

$$F[f]=\int_{S_2}d^2u\,f(\boldsymbol{u})\ln[f(\boldsymbol{u})/f_{\mathrm{eq}}(\boldsymbol{u})]. \tag{12}$$

In terms of F, the kinetic equation (1) can be rewritten as

$$\tau\partial_t f=-\mathrm{P\acute{e}}\boldsymbol{\mathcal{L}}\cdot[(\tilde{\boldsymbol{\Omega}}+B\boldsymbol{u}\times\tilde{\boldsymbol{D}}\cdot\boldsymbol{u})f]+\frac{1}{2}\boldsymbol{\mathcal{L}}\cdot f\boldsymbol{\mathcal{L}}\frac{\delta F[f]}{\delta f}, \tag{13}$$

where $\delta/\delta f$ denotes the Volterra functional derivative. The time rate of change of the free energy functional (12) is given by

$$\tau\dot{F}=\frac{1}{nk_{\mathrm{B}}T}[\boldsymbol{t}^{\mathrm{a}}\cdot\tilde{\boldsymbol{\Omega}}+\boldsymbol{T}^{\mathrm{pot}}:\tilde{\boldsymbol{D}}]-\frac{1}{2}\langle\boldsymbol{s}^2\rangle, \tag{14}$$

where we used Eq. (1) and introduced quantities $\boldsymbol{t}^{\mathrm{a}}$ and $\boldsymbol{s}$ by $\boldsymbol{T}^{\mathrm{a}}=\boldsymbol{\epsilon}\cdot\boldsymbol{t}^{\mathrm{a}}$ and $\boldsymbol{s}=\boldsymbol{\mathcal{L}}(\delta F/\delta f)$. In the absence of flow, Eq. (14) proves that the free energy functional (12) is nonincreasing, $\dot{F}\leqslant0$, due to the dynamics (1), with $\dot{F}=0$ in equilibrium.

In the presence of a steady potential flow, the same arguments can be applied to the functional F_{s}, that is obtained by replacing the equilibrium distribution function f_{eq} in Eq. (12) by the steady state distribution f_{s}, given by Eq. (11).

C. Moment equations

From the kinetic equation (1), the dynamics of the kth moment $\langle u_{\alpha_1}\cdots u_{\alpha_k}\rangle$ is obtained,

$$\begin{aligned}\tau\partial_t\langle u_{\alpha_1}\cdots u_{\alpha_k}\rangle &=-\mathrm{P\acute{e}}\sum_{j=1}^{k}\tilde{\Omega}_{\alpha}\epsilon_{\alpha\alpha_j\beta}\left\langle u_\beta\prod_{\substack{i=1\\i\neq j}}^{k}u_{\alpha_i}\right\rangle\\ &+\mathrm{P\acute{e}}B\left[\sum_{j=1}^{k}\tilde{D}_{\alpha_j\beta}\left\langle u_\beta\prod_{\substack{i=1\\i\neq j}}^{k}u_{\alpha_i}\right\rangle-k\tilde{D}_{\alpha\beta}\left\langle u_\alpha u_\beta\prod_{i=1}^{k}u_{\alpha_i}\right\rangle\right]-\frac{k(k+1)}{2}\langle u_{\alpha_1}\cdots u_{\alpha_k}\rangle\\ &+\sum_{\substack{j,l=1\\j>l}}^{k}\delta_{\alpha_j\alpha_l}\left\langle\prod_{\substack{i=1\\i\neq j,l}}^{k}u_{\alpha_i}\right\rangle-\frac{k}{2}h_\beta\left\langle u_\beta\prod_{i=1}^{k}u_{\alpha_i}\right\rangle\\ &+\frac{1}{2}\sum_{j=1}^{k}h_{\alpha_j}\left\langle\prod_{\substack{i=1\\i\neq j}}^{k}u_{\alpha_i}\right\rangle.\end{aligned} \tag{15}$$

The equation for the first moment, $k=1$, is therefore

$$\tau\partial_t\langle \boldsymbol{u}\rangle = \mathrm{P\acute{e}}\tilde{\boldsymbol{\Omega}}\times\langle \boldsymbol{u}\rangle + \mathrm{P\acute{e}}B\langle(\mathbf{1}-\boldsymbol{uu})\boldsymbol{u}\rangle:\tilde{\boldsymbol{D}} - \langle \boldsymbol{u}\rangle + \frac{1}{2}(\mathbf{1}-\langle \boldsymbol{uu}\rangle)\cdot\boldsymbol{h}, \tag{16}$$

and for the second, $k=2$,

$$\tau\partial_t\langle \boldsymbol{uu}\rangle = \mathrm{P\acute{e}}(\tilde{\boldsymbol{W}}\cdot\langle \boldsymbol{uu}\rangle - \langle \boldsymbol{uu}\rangle\cdot\tilde{\boldsymbol{W}}) + \mathrm{P\acute{e}}\,B[\tilde{\boldsymbol{D}}\cdot\langle \boldsymbol{uu}\rangle + \langle \boldsymbol{uu}\rangle\cdot\tilde{\boldsymbol{D}} - 2\tilde{\boldsymbol{D}}:\langle \boldsymbol{uuuu}\rangle] - 3\langle\overline{\boldsymbol{uu}}\rangle - \boldsymbol{h}\cdot\langle \boldsymbol{uuu}\rangle + \frac{1}{2}(\boldsymbol{h}\langle \boldsymbol{u}\rangle + \langle \boldsymbol{u}\rangle\boldsymbol{h}), \tag{17}$$

where $\tilde{\boldsymbol{W}}=\boldsymbol{\epsilon}\cdot\tilde{\boldsymbol{\Omega}}$.

Using Eq. (17), the explicit contribution of the potential V to the symmetric stress tensor (6) can be eliminated [20],

$$\boldsymbol{T}^{\mathrm{s}} = 2\eta_{\mathrm{s}}(1+5\phi Q_1)\boldsymbol{D} + 5\eta_{\mathrm{s}}\phi\{2Q_3(\boldsymbol{D}\cdot\langle \boldsymbol{uu}\rangle + \langle \boldsymbol{uu}\rangle\cdot\boldsymbol{D}) - Q_{23}\boldsymbol{D}:\langle \boldsymbol{uuuu}\rangle + Q_0[\tilde{\boldsymbol{W}}\cdot\langle \boldsymbol{uu}\rangle - \langle \boldsymbol{uu}\rangle\cdot\tilde{\boldsymbol{W}} - \partial_t\langle \boldsymbol{uu}\rangle]\}. \tag{18}$$

Similarly, with the help of the moment equation (16), the explicit dependence on the potential can be eliminated from the antisymmetric stress tensor (4), $\boldsymbol{h}=\boldsymbol{\Pi}^{-1}\cdot\boldsymbol{a}$, with

$$\boldsymbol{a} = \tau\partial_t\langle \boldsymbol{u}\rangle - \mathrm{P\acute{e}}\tilde{\boldsymbol{\Omega}}\times\langle \boldsymbol{u}\rangle - \mathrm{P\acute{e}}B[\tilde{\boldsymbol{D}}\cdot\langle \boldsymbol{u}\rangle - \langle \boldsymbol{uuu}\rangle:\tilde{\boldsymbol{D}}] + \langle \boldsymbol{u}\rangle, \tag{19}$$

where $\boldsymbol{\Pi}^{-1}$ denotes the inverse of the matrix $\boldsymbol{\Pi}\equiv(\mathbf{1}-\langle \boldsymbol{uu}\rangle)$.

In the absence of potential forces and for $\mathrm{P\acute{e}}\to 0$, the steady state stress tensor $\boldsymbol{T}$ reduces to $\boldsymbol{T}=2\eta_{0,r}\boldsymbol{D}$, with the zero-shear viscosity of a dilute suspension of magnetically neutral ellipsoidal particles (axis ratio r),

$$\eta_{0,r} = \eta_{\mathrm{s}} + \eta_{0,r}^{\phi},$$

$$\eta_{0,r}^{\phi} \equiv \phi\{5Q_1 + (2Q_3 - Q_2)\}\eta_{\mathrm{s}},$$

$$\to \eta_0^{\phi} \equiv \eta_{0,r=1}^{\phi} = \frac{5}{2}\phi\eta_{\mathrm{s}}. \tag{20}$$

Einstein's formula $\eta_0\equiv\eta_{0,r=1}=(1+5\phi/2)\eta_{\mathrm{s}}$ is recovered from this expression for spherical particles (see Appendix C). Results for the viscosity coefficients below will be related to the concentration-induced increase of the zero-shear-rate viscosity η_0^{ϕ} for spheres, i.e., we eventually use the identities $n\zeta_{\mathrm{rot}}=2nk_{\mathrm{B}}T\tau=(12\eta_0^{\phi}/5)e_r$ in order to make the dependence on shape evident. We generally omit the second index r for quantities, if $r=1$.

Due to the hydrodynamic drag and the magnetic field, the equation for the moment of order k, Eq. (15), couples to moments of order $k\pm1$ and $k\pm2$ $(k\geqslant 0)$. Therefore, a finite set of closed equations for the macroscopic magnetization and the macroscopic stress tensor $\boldsymbol{T}$ cannot in general be derived from the kinetic model unless some approximations are invoked.

III. RESULTS FOR UNIAXIAL SYMMETRY

In order to obtain more explicit expressions for the stress tensor and the viscosity coefficients, we here propose to consider the class of uniaxial distribution functions. This approach was applied successfully in Ref. [19] to dilute suspensions of spherical ferromagnetic particles. In the present case, in analogy to Ref. [20], further manipulations are based on the expressions (8) and (18) for the antisymmetric and symmetric part of the stress tensor. It should be mentioned that alternative and nonequivalent approaches for deriving viscosity coefficients within the uniaxial assumption are possible. For example, using this assumption for the formulation (6), (9), and (18) of the symmetric stress tensor yields different results which, for comparison, are presented in Sec. III B. By comparison with numerical simulations of the full kinetic model, however, use of the results in Sec. III B is discouraged, while those presented in the following section show rather good agreement.

Uniaxial symmetry of the distribution function with respect to the director $\boldsymbol{n}$ is defined here as $f(\boldsymbol{u};t)=f_{\mathrm{uni}}(\boldsymbol{u}\cdot\boldsymbol{n};t)$. Therefore f has the representation

$$f_{\mathrm{uni}}(\boldsymbol{u}\cdot\boldsymbol{n}) = \frac{1}{4\pi}\sum_{j=0}^{\infty}\frac{1}{2j+1}S_jP_j(\boldsymbol{u}\cdot\boldsymbol{n}), \tag{21}$$

with the scalar order parameters $S_j=\langle P_j(\boldsymbol{u}\cdot\boldsymbol{n})\rangle$, and P_j are Legendre polynomials. The moments of the distribution function $\langle \boldsymbol{u}\rangle,\langle \boldsymbol{uu}\rangle$, etc., can be expressed in terms of the director $\boldsymbol{n}$ and the order parameters S_i (expressions are collected in Appendix E). The S_j are bounded, $0\leqslant S_1\leqslant 1$ and $-1/2\leqslant S_j\leqslant 1$ for $j>1$.

In particular, the equilibrium distribution, Eq. (10), shows uniaxial symmetry around the direction of the magnetic field, $\boldsymbol{n}^{\mathrm{eq}}=\hat{\boldsymbol{h}}$. In the equilibrium state, the orientational order parameters $S_j^{\mathrm{eq}}=L_j(h)$ can be calculated explicitly as a function of the magnetic field,

$$L_j(h)\equiv\langle P_j(\boldsymbol{u}\cdot\boldsymbol{n})\rangle_{\mathrm{eq}} = \frac{I_{j+1/2}(h)}{I_{1/2}(h)}, \tag{22}$$

where $I_{j+1/2}$ is a modified spherical Bessel function [1]. The functions $L_j(h)$ satisfy the recursion relation

$$L_{j+1}(h) = L_{j-1}(h) - \frac{2j+1}{h}L_j(h), \tag{23}$$

with $L_0=1$ and $L_1(h)$ is identical to the Langevin function $L(h)$. In equilibrium, Eqs. (E1)–(E4) reduce to the expressions for the equilibrium moments, given, e.g., in Ref. [1].

For spherical particles, we have shown in Ref. [19], that the assumption of uniaxial symmetry leads to very accurate results also out of equilibrium, even if the actual distribution function is not strictly uniaxial symmetric. The validity of the assumption of uniaxial symmetry for nonspherical particles is discussed in Sec. V.

Inserting relations (E1)–(E4) valid in the uniaxial phase into Eq. (16), the following time evolution equations for the orientational order parameter S_1 and the balance equation for the director are obtained:

$$\dot{S}_1=\frac{3}{5}B(S_1-S_3)(\boldsymbol{D}:\boldsymbol{nn})-2D_rS_1+\frac{2}{3}D_r(1-S_2)(\boldsymbol{h}\cdot\boldsymbol{n}), \quad (24)$$

$$(\mathbf{1}-\boldsymbol{nn})\cdot\left[D_r\boldsymbol{h}-\frac{3S_1}{2+S_2}\boldsymbol{N}+B\frac{3(3S_1+2S_3)}{5(2+S_2)}\boldsymbol{D}\cdot\boldsymbol{n}\right]=\mathbf{0}. \quad (25)$$

From Eqs. (E1)–(E4),(18), the symmetric stress tensor (6) is found to be of the form (A4) assumed in the Ericksen-Leslie theory if the viscosity coefficients are identified with (see also Ref. [20])

$$\alpha_1=-2\,\eta_0^{\phi}Q_{23}S_4, \quad (26)$$

$$\alpha_2+\alpha_3=-4\,\eta_0^{\phi}Q_0S_2, \quad (27)$$

$$\alpha_4-2\,\eta_{0,r}=-4\,\eta_0^{\phi}\left[\frac{2}{7}Q_{32}S_2+\frac{3}{35}Q_{23}S_4\right], \quad (28)$$

$$\alpha_5+\alpha_6=\frac{16}{35}\,\eta_0^{\phi}[3Q_{32}S_2+Q_{23}S_4]. \quad (29)$$

Equation (25) is of the general form of the balance equation for the director assumed in the Ericksen-Leslie theory (A3). The viscosity coefficients γ_1 and γ_2 can be extracted from Eq. (25) only up to an undetermined factor that relates the magnetic field $\boldsymbol{h}$ with the external director body force $\boldsymbol{h_n}$ appearing in the Ericksen-Leslie theory (A3). However, inserting Eqs. (E1), (E2), (E3), and (16) into the antisymmetric stress tensor (8), we recover the Ericksen-Leslie form for $\boldsymbol{T}^{\mathrm{a}}$ (A4) with the viscosity coefficients ($\Gamma\equiv 12\,\eta_0^{\phi}e_r/5=6\,\eta_s\phi e_r$)

$$\gamma_1=\Gamma\frac{3S_1^2}{2+S_2}, \quad \gamma_2=-\Gamma B\frac{3S_1(3S_1+2S_3)}{5(2+S_2)}. \quad (30)$$

For spherical particles, $B=0$,$e_r=1$, we recover the result obtained in Ref. [19]. Equation (30) introduces also the viscosity coefficient γ_2, which is absent in the kinetic model introduced in Ref. [4]. In the context of molecular liquids and in liquid crystals, this term is known to be responsible for the flow alignment phenomenon [22,23]. In case of random alignment, $S_i=0$, we find no contribution to the antisymmetric stress tensor, $\gamma_i=0$, while in the opposite limit of perfect alignment, $S_i=1$, the maximum values $\gamma_1=\Gamma$ and $\gamma_2=B\Gamma$ are attained. Comparison of Eqs. (25) and (30) with Eq. (A3) allows us to identify the director body force, $\boldsymbol{h_n}=nk_{\mathrm{B}}TS_1\boldsymbol{h}$.

Note that the parameters α_4 and γ_1, given by Eqs. (28) and (30), are positive as required from dissipation arguments (A6). The parameters α_i and γ_i also obey the restriction (A7).

According to our result stated in Eq. (30), the enhancement of the the rotational viscosity for nonspherical units is just given by the quantity e_r characterizing the shape alone [Eq. (B3)]. While $e_{r=1}=1$, for an axis ratio of $r=10$ we predict an increase in γ_1 by about 800%.

For later use, we provide the ratio of the coefficients γ_i,

$$\lambda_{\mathrm{t}}\equiv-\frac{\gamma_2}{\gamma_1}=\frac{B(3S_1+2S_3)}{5S_1}. \quad (31)$$

As will be discussed in Sec. III C, $|\lambda_{\mathrm{t}}|<1$ implies director tumbling in steady shear flow, while $|\lambda_{\mathrm{t}}|\geqslant 1$ implies the existence of a steady solution if the magnetic field is absent.

From Eq. (24), also the angle φ between the direction of the magnetic field and the magnetization can be calculated,

$$\cos\varphi\equiv\hat{\boldsymbol{h}}\cdot\boldsymbol{n}=\frac{3S_1}{h(1-S_2)}\left[1-\frac{3B(S_1-S_3)}{5S_1}\mathrm{Pé}(\tilde{\boldsymbol{D}}:\boldsymbol{nn})\right]. \quad (32)$$

Equation (32) generalizes the corresponding result for spheres, $B=0$, obtained in Ref. [19]. The additional term is responsible for the flow alignment of nonspherical particles.

A. Small Péclet number

In the low Péclet number regime Pé$\ll$1, the order parameters S_i may be replaced by their equilibrium values S_i^{eq}. Thus, the alignment angle φ, given by Eq. (32), becomes

$$\cos\varphi^0=1-\frac{3BL_2(h)}{hL_1(h)}\mathrm{Pé}(\tilde{\boldsymbol{D}}:\boldsymbol{nn}), \quad (33)$$

and $\varphi^0\to 0$ as Pé$\to 0$. As expected, a perfect alignment of the direction of magnetization with the magnetic field is obtained in this regime, $\boldsymbol{n}=\hat{\boldsymbol{h}}$.

The corresponding form of the stress tensor (A1) with $\boldsymbol{n}=\hat{\boldsymbol{h}}$ reads

$$\boldsymbol{T}^0=\alpha_1^0(\hat{\boldsymbol{h}}\hat{\boldsymbol{h}}:\boldsymbol{D})\hat{\boldsymbol{h}}\hat{\boldsymbol{h}}+\alpha_2^0\hat{\boldsymbol{h}}\boldsymbol{N}+\alpha_3^0\boldsymbol{N}\hat{\boldsymbol{h}}+\alpha_4^0\boldsymbol{D}\alpha_5^0\hat{\boldsymbol{h}}\hat{\boldsymbol{h}}\cdot\boldsymbol{D}+\alpha_6^0\boldsymbol{D}\cdot\hat{\boldsymbol{h}}\hat{\boldsymbol{h}} \quad (34)$$

and has been obtained previously in Refs. [12,13] from the kinetic model (1) in the limit Pé$\to 0$. The viscosity coefficients α_i^0 are obtained from Eqs. (26)–(30), by replacing S_i with their equilibrium values S_i^{eq},

$$\alpha_1^0=-2\,\eta_0^{\phi}Q_{23}L_4(h), \quad (35)$$

$$\alpha_2^0+\alpha_3^0=-4\,\eta_0^{\phi}Q_0L_2(h), \quad (36)$$

$$\alpha_4^0-2\,\eta_{0,r}=-4\,\eta_0^{\phi}\left[\frac{2}{7}Q_{32}L_2(h)+\frac{1}{35}Q_{23}L_4(h)\right], \quad (37)$$

$$\alpha_5^0+\alpha_6^0=\frac{8}{7}\,\eta_0^{\phi}\left[2Q_3L_2(h)-2Q_{23}\frac{L_3(h)}{h}\right]. \quad (38)$$

For the viscosity coefficients $\gamma_1^0=\alpha_3^0-\alpha_2^0$ and $\gamma_2^0=\alpha_6^0-\alpha_5^0$ we find

$$\gamma_1^0=\Gamma\frac{hL^2(h)}{h-L(h)}, \quad (39)$$

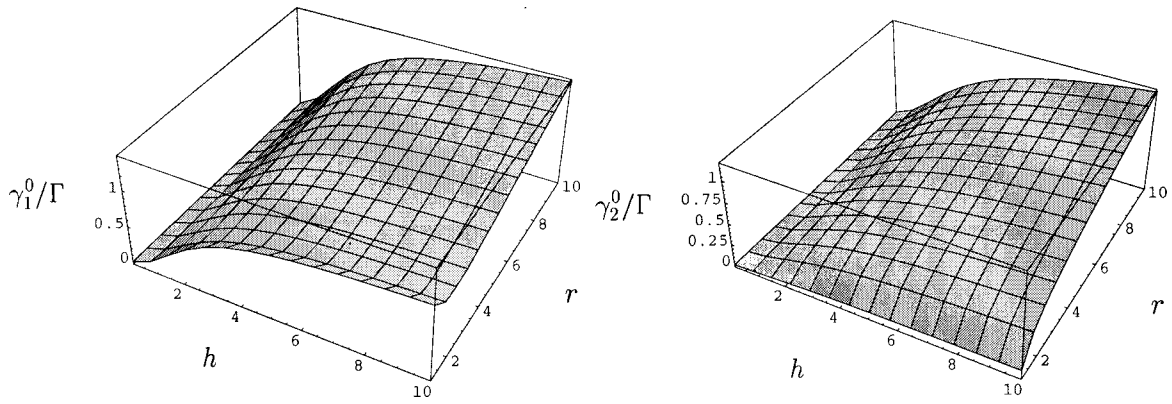

FIG. 1. Reduced rotational viscosities γ_1^0/Γ and $\gamma_2^0/(B\Gamma)$, given by Eqs. (39) and (40) as a function of the dimensionless magnetic field (Langevin parameter) $h=\mu H/k_BT$ and axis ratio r of the ellipsoid.

$$\gamma_2^0=-\Gamma B\frac{L(h)[(6+h^2)L(h)-2h]}{h[h-L(h)]}. \tag{40}$$

The expressions for the viscosity coefficients α_i^0 given in Refs. [12,13] differ, however, from these results. As pointed out in Ref. [13], viscous contributions to the stress tensor are neglected in Ref. [12] and therefore agreement with that result should not be expected. Expressions (35)–(40) also disagree with the result in Ref. [13], which were obtained with the help of an ansatz for the linearized, stationary distribution function in the limit Pé$\to$0. In case of spherical particles, the expression (39) with $\Gamma=6\eta_s\phi$ was already derived in Ref. [4] and found to agree with the exact expression in the limit Pé$\to$0 within 3% [24]. However, comparison to the tabulated values of γ_1^0 in Ref. [13] yields discrepancies of the order 10%. Therefore, no further comparison to results in Ref. [13] is made in the sequel.

In Fig. 1, the viscosity coefficients γ_1^0,γ_2^0, given by Eqs. (39) and (40), are shown as a function of the magnetic field h and the axis ratio of the ellipsoid r. The coefficients γ_1^0,γ_2^0 are normalized by their maximum values. From Fig. 1 it is seen that the values of the viscosities increase with increasing r, the limit $r\to1$ corresponding to the result for spherical particles.

B. Parodi's relation and an alternative set of viscosity coefficients

For small Péclet numbers, the stress tensor $\boldsymbol{T}$ is a linear tensor function of the symmetric and antisymmetric velocity gradient, given by Eq. (34). Employing Onsager's reciprocity relation, the matrix providing the linear relation between the stress tensor and the velocity gradient is assumed to be symmetric. In the present case, this relation is known as Parodi's relation [23],

$$\alpha_2^0+\alpha_3^0=\gamma_2^0. \tag{41}$$

The validity of Parodi's relation in the description of liquid-crystalline polymers has frequently been discussed in the literature [20,23]. From Eqs. (36) and (40) it is seen that Parodi's relation is not satisfied identically except in the limit $S_i\to1$, i.e., $h\to\infty$. Note, that in this regime the assumption of uniaxial symmetry is most likely valid.

The violation of Eq. (41) for finite h might be considered as a drawback of the preceeding approximation. Although one should remember that the assumption of uniaxial symmetry is in general not satisfied strictly by the underlying kinetic model. The violation of Parodi's relation stems from the different treatment of the symmetric and antisymmetric stress tensor in the above derivation: the first-moment equation is used for the formulation of the antisymmetric stress tensor and the second-moment equation for the symmetric stress tensor. Since we require the limit of spherical particles, $B=0$, to be given by γ_1, Eq. (30) in accordance with previous results [4], Parodi's relation can be preserved if the first-moment equation is considered only and no use of Eq. (18) is made. If the magnetic field is eliminated from Eq. (9) with the help of Eq. (19), the resulting stress tensor is given by the Ericksen-Leslie form (A4) with an additional term $\beta\boldsymbol{nn}$. Since $\beta\to0$ for Pé$\ll1$, the original Ericksen-Leslie form (A4) is restored for small Péclet numbers. The coefficients γ_1,γ_2 are again given by Eq. (30). The coefficients appearing in the symmetric stress tensor differ, however, from Eqs. (26)–(29),

$$\alpha_1^P=-2\eta_0^\phi(Q_{23}-2BQ_0)S_4-\frac{3}{5}\Gamma\frac{B^2}{2+S_2}\Big[S_3(3S_1+2S_3)+\frac{3(S_1-S_3)}{10(1-S_2)}(10S_3-9S_1S_2-S_2S_3)\Big], \tag{42}$$

$$\alpha_2^P+\alpha_3^P=\gamma_2, \tag{43}$$

$$\alpha_4^P-2\eta_{0,r}^P=\frac{4}{7}\eta_0^\phi\Big[(2Q_{32}+BQ_0)S_2+\frac{1}{5}(Q_{23}-2BQ_0)S_4\Big], \tag{44}$$

$$\alpha_5^P+\alpha_6^P=\frac{4}{7}\eta_0^\phi[3(2Q_{32}-BQ_0)S_2+2(Q_{23}-2BQ_0)S_4]+\gamma_2\lambda_t, \tag{45}$$

where the zero-shear viscosity is given by $\eta_{0,r}^{\mathrm{P}}=\eta_s+\eta_{0,r}^{\mathrm{P},\phi}$ with $\eta_{0,r}^{\mathrm{P},\phi}=\eta_0^{\phi}[Q_1+((3/2)Q_3-Q_2-BQ_0)/5]$ and η_0^{ϕ} is given by the last of Eqs. (20). Diagonal contributions to the stress tensor have again be omitted since we consider incompressible conditions. From Eq. (43) it is seen that Parodi's relation (41) is satisfied and holds for arbitrary Péclet numbers. Comparison of Eqs. (26)–(29) and (42)–(45) together with Eq. (30) are compared in Sec. V with the result of Brownian dynamics simulations of the full kinetic model for steady shear flows. We will show that the agreement is better for the first set of viscosity coefficients [Eqs. (26)–(29), (30)] than the second [Eqs. (42)–(45), (30)]. Thus, violations of uniaxial symmetry by the kinetic model seem to be better approximated if the assumption of uniaxial symmetry is imposed on the form (18) of the symmetric stress tensor than on the definition (6).

C. Steady shear flow

In this section, the previous results are applied to the important situation of a steady laminar shear flow between two parallel plates. The notion of the Miesowicz viscosities is introduced. Let the flow be oriented along the x direction and the gradient in y direction, $\boldsymbol{v}=[v(y),0,0]$.

If the local magnetic field $\boldsymbol{h}$ lies in the plane of shear, the magnetic field and the director can be written as

$$\boldsymbol{h}=h(\cos\vartheta,\sin\vartheta,0),\quad \boldsymbol{n}=(\cos\theta,\sin\theta,0), \tag{46}$$

where ϑ is the angle between the magnetic field and the flow direction and θ is the angle between the director and hence the magnetization and the x direction. Thus, the alignment angle φ, introduced above, is given by $\varphi=\vartheta-\theta$. In the steady state, the momentum balance (A2) becomes

$$g(\theta)\dot{\gamma}=\frac{dp}{dx}y+\sigma, \tag{47}$$

where $\dot{\gamma}=dv/dy$ and σ is the constant shear stress applied to the fluid and

$$g(\theta)=\frac{1}{2}[2\alpha_1\sin^2\theta\cos^2\theta+(\alpha_5-\alpha_2)\sin^2\theta+(\alpha_6+\alpha_3)\cos^2\theta+\alpha_4]. \tag{48}$$

If there is no pressure gradient and the flow is caused by one plate moving at uniform velocity parallel to its own plane we have $dp/dx=0$ and $\sigma\neq 0$. On the other hand, if the plates are at rest and taking $y=0$ at the center between the plates gives $dp/dx\neq 0$ and $\sigma=0$.

In the present flow situation, the balance equation for the director, Eq. (25), becomes

$$\mathrm{Mn}(\tilde{\gamma}_1+\tilde{\gamma}_2\cos 2\theta)+\frac{1}{2}\sin(\vartheta-\theta)=0, \tag{49}$$

where the Mason number $\mathrm{Mn}=\tau\dot{\gamma}/h$ and dimensionless viscosities $\tilde{\gamma}_i\equiv\gamma_i/\Gamma$, $i=1,2$, have been used. Equations (47) and (49) can be solved to give the alignment angle and the velocity gradient. If the plates are separated far enough, which we assume in the following, boundary effects can be neglected.

In the absence of a magnetic field, the orientation angle approaches the stationary value θ_0 defined by

$$\cos(2\theta_0)=-\gamma_1/\gamma_2\equiv 1/\lambda_t. \tag{50}$$

The interpretation of λ_t as tumbling parameter stems from Eq. (50) which has no solution for $|\lambda_t|<1$. Therefore, in the absence of a magnetic field, $|\lambda_t|<1$ implies director tumbling while $|\lambda_t|>1$ allows for a steady solution [23].

If the magnetization (and not necessarily the magnetic field) is oriented parallel to the flow ($\sin\theta=0$) and gradient ($\cos\theta=0$) direction, the so-called Miesowicz (shear) viscosities η_1,η_2 are measured, respectively, with $2\eta_1=\alpha_3+\alpha_4+\alpha_6$ and $2\eta_2=-\alpha_2+\alpha_4+\alpha_5$. Since these viscosities are predicted to depend on the shape of the ferromagnetic units, we will systematically label them with a second index (r) in the following. By using Eqs. (48) and (26)–(30) we obtain

$$\eta_{1,r}=\eta_{0,r}+2\eta_0^{\phi}\left[\frac{3e_r}{10}\frac{3S_1^2}{2+S_2}(1-\lambda_t)+\frac{1}{7}\left(Q_{32}-\frac{7}{2}Q_0\right)S_2+\frac{4}{35}Q_{23}S_4\right], \tag{51}$$

$$\eta_{2,r}=\eta_{0,r}+2\eta_0^{\phi}\left[\frac{3e_r}{10}\frac{3S_1^2}{2+S_2}(1+\lambda_t)+\frac{1}{7}\left(Q_{32}+\frac{7}{2}Q_0\right)S_2+\frac{4}{35}Q_{23}S_4\right]. \tag{52}$$

If the magnetization is oriented parallel to the flow vorticity, the Miesowicz viscosity $\eta_3=\alpha_4/2$ is measured,

$$\eta_{3,r}=\eta_{0,r}-\frac{4}{7}\eta_0^{\phi}\left[Q_{32}S_2+\frac{1}{10}Q_{23}S_4\right]. \tag{53}$$

A fourth viscosity coefficient η_{12} has been introduced in order to fully characterize the shear viscosity,

$$\eta_{12}=4\eta_{45}-2(\eta_1+\eta_2)=\alpha_1,$$

where η_{45} is the viscosity with the director parallel to the bisector between the x and y axis. From Eqs. (51) and (52) the difference of the Miesowicz viscosities is found to be given by

$$\eta_{2,r}-\eta_{1,r}=2\eta_0^{\phi}\left[\frac{3e_r}{5}\frac{3S_1^2}{2+S_2}\lambda_t+Q_0S_2\right]. \tag{54}$$

In Sec. V, also the (experimentally more important) viscosity coefficients η_a, η_b, and η_c are considered that are measured if the magnetic field (and not necessarily the magnetization) is oriented in flow, gradient, and vorticity direction, respectively. The viscosity coefficients η_a, η_b, and η_c agree with η_1, η_2, and η_3 only in the limit Pé$\ll 1$, see Sec. III A.

From the Miesowicz viscosity coefficients the so-called McTague [1] viscosity coefficients are found,

$$\eta_{\parallel}=\eta_{1,r}, \quad \eta_{\perp}=(\eta_{2,r}+\eta_{3,r})/2, \tag{55}$$

which are measured in a pipe flow, if the magnetization is oriented in flow and perpendicular to the flow direction, respectively. For spherical particles, $B=0$, one obtains $\eta_{\parallel}=\eta_0$ and $\eta_{\perp}=\eta_0+\gamma_1/4$, where $\eta_0=\eta_{0,r=1}=\eta_s+\eta_0^{\phi}$ is the viscosity of a dilute suspension of magnetically neutral spherical particles.

Dilute suspensions of nonspherical particles also show normal stress effects. The first normal stress coefficient N_1 for the shear flow $\boldsymbol{v}=[v(y),0,0]$ is defined as $N_1=(T_{yy}-T_{xx})/\dot{\gamma}$, with $\dot{\gamma}=dv(y)/dy$. Analogously, the second normal stress coefficient N_2 is defined as $N_2=(T_{zz}-T_{yy})/\dot{\gamma}$. For the geometry described by Eq. (46), these coefficients can be written as

$$N_1=\frac{1}{2}[\alpha_1\cos(2\theta)+(\alpha_2+\alpha_3)]\sin(2\theta), \tag{56}$$

$$-N_2=\frac{1}{4}[\alpha_1\sin^2\theta+\alpha_2+\alpha_3+\alpha_5+\alpha_6]\sin(2\theta). \tag{57}$$

Note that the normal stress coefficients N_1, N_2 vanish for perfect orientation in either flow or gradient direction.

D. Small Mason number

For small Mason numbers, $\mathrm{Mn}\ll 1$, the dynamics is dominated by the magnetic field. For $\mathrm{Mn}=0$, the stationary value $\theta_0=\vartheta$ is found from Eq. (49). This corresponds to perfect alignment of the director with the external magnetic field. In case of nonvanishing but small Mason number, $\mathrm{Mn}\ll 1$, the alignment angle is obtained from Eq. (49) as $\theta=\theta_0+\mathrm{Mn}\theta_1+O(\mathrm{Mn}^2)$, with the first-order contribution

$$\theta_1=\tilde{\gamma}_1+\tilde{\gamma}_2\cos 2\vartheta. \tag{58}$$

In the limit of perfect orientation, $S_i=1$, θ_1 becomes $\theta_1=1+B\cos 2\vartheta$, while $\theta_1=0$ for isotropic states. With the help of the alignment angle θ, the normal stress coefficient N_1 given by Eq. (56) becomes

$$N_1=\begin{cases}\mathrm{Mn}(\tilde{\gamma}_1-\tilde{\gamma}_2)(-\alpha_1+\alpha_2+\alpha_3) & \text{for} \quad \vartheta=\pi/2,\\ 2\mathrm{Mn}(\tilde{\gamma}_1+\tilde{\gamma}_2)(\alpha_1+\alpha_2+\alpha_3) & \text{for} \quad \vartheta=0,\end{cases} \tag{59}$$

if the magnetic field is oriented in the gradient ($\vartheta=\pi/2$) or velocity ($\vartheta=0$) direction.

In the low Péclet number regime, the order parameters S_i can be replaced by their equilibrium values S_i^{eq}. Thus, the Miesowicz viscosities $\eta_{i,r}$ given by Eqs. (51), (52), (53) become explicit functions of the magnetic field h and the axis ratio r. Figure 2 shows the reduced Miesowicz viscosities $\Delta\tilde{\eta}_i^0\equiv(\eta_{i,r}^0-\eta_{0,r})/2\eta_0^{\phi}$, that result upon the replacement $S_i\to S_i^{\mathrm{eq}}$ in Eqs. (51), (52), (53). Experimental results are most commonly given in terms of the relative shear viscosity change, which in case $\mathrm{Pé}\ll 1$ is related to $\Delta\tilde{\eta}_i^0$ by

$$R_i^0\equiv\frac{\eta_{i,r}^0-\eta_{0,r}}{\eta_{0,r}}=\Delta\tilde{\eta}_i^0\frac{5\phi}{1+\eta_{0,r}^{\phi}/\eta_s}. \tag{60}$$

Note that within the present model $\Delta\tilde{\eta}_i^0$ is independent of the volume fraction ϕ which is not the case for R_i^0. In the limit of strong magnetic field, $\mathrm{Mn}\ll 1$, the magnetic moments are perfectly oriented, $S_i\to 1$. In this case, the Miesowicz viscosities (51), (52), and (53) approach their limiting values

$$\eta_{1,r}^{\infty}=\eta_{0,r}+2\eta_0^{\phi}\left[\frac{3e_r}{10}(1-2B)+\frac{1}{5}(Q_2+3Q_3)\right], \tag{61}$$

$$\eta_{2,r}^{\infty}=\eta_{0,r}+2\eta_0^{\phi}\left[\frac{3e_r}{10}(1+2B)+\frac{1}{5}(Q_2+3Q_3)\right], \tag{62}$$

$$\eta_{3,r}^{\infty}=\eta_{0,r}+2\eta_0^{\phi}\left[\frac{1}{5}(Q_2-2Q_3)\right], \tag{63}$$

with $\eta_{i,r}\to\eta_{i,r}^{\infty}+O(h^{-1})$ as $S_i\to 1$. It is interesting to note from Eqs. (62) and (63) that $\eta_{2,r}^{\infty}>\eta_{0,r}$ and $\eta_{3,r}^{\infty}<\eta_{0,r}$, while from Eq. (61) one finds, that $\eta_{1,r}^{\infty}>\eta_{0,r}$ for $r<r_{\mathrm{crit}}$ and $\eta_{1,r}^{\infty}<\eta_{0,r}$ for $r>r_{\mathrm{crit}}$, with $r_{\mathrm{crit}}\approx 1.96$. From Eqs. (61)–(63) the inequality $\eta_{2,r}^{\infty}\geqslant\eta_{1,r}>\eta_{3,r}$ is verified with $\eta_{2,r}^{\infty}=\eta_{1,r}$ for $r=1$. We mention that $\eta_{2,r}^{\infty}\geqslant\eta_{1,r}$ is in agreement with the results of nonequilibrium molecular dynamics simulations of a fully oriented model ferrofluid if the magnetic interactions of the colloidal particles are strong enough [25].

For weak magnetic field, $h\ll 1$, expanding $\eta_{i,r}^0$ in powers of the Langevin parameter h leads to

$$\eta_{i,r}^0=\eta_{0,r}+2\eta_0^{\phi}c_ih^2+O(h^3) \quad \text{for} \quad h\to 0, \tag{64}$$

where the coefficients c_i depend only on the axis ratio r, $c_1=c-Q_0(1-1/B)/12$, $c_2=c+Q_0(1+1/B)/12$, and $c_3=-2c$, where $c=Q_{32}/105$. For $\eta_{2,r}$, the quadratic behavior predicted in Eq. (64) is seen in recent experiments on a commercial ferrofluid [3].

Denoting the reduced McTague viscosity coefficients by $\Delta_X=[\eta_{X,r}(h)-\eta_{X,r}(h=0)]/\eta_{X,r}(h=0)$, $X=\parallel,\perp$, we notice that $\Delta_{\parallel}$ changes by approximately 30% and $\Delta_{\perp}$ by almost 400% for $h\approx 10$ and $r\approx 10$.

IV. EFFECTIVE FIELD APPROXIMATION

The so-called quasi-equilibrium approximation (QEA) is a powerful tool to derive macroscopic equations from kinetic models [26–28]. Note, that in the context of ferrofluids, the term ''quasi-equilibrium approximation'' is sometimes used for the special approximation of neglecting magnetic relaxation processes [1]. Here, the term QEA is used in its broad sense, as is common in many branches of statistical physics (see, e.g., [26,27] and references therein). Note, that ''quasi'' does not imply ''near.''

As set of macroscopic variables we choose the first moment of the distribution function, $\boldsymbol{A}=\langle\boldsymbol{u}\rangle$. The QEA is ob-

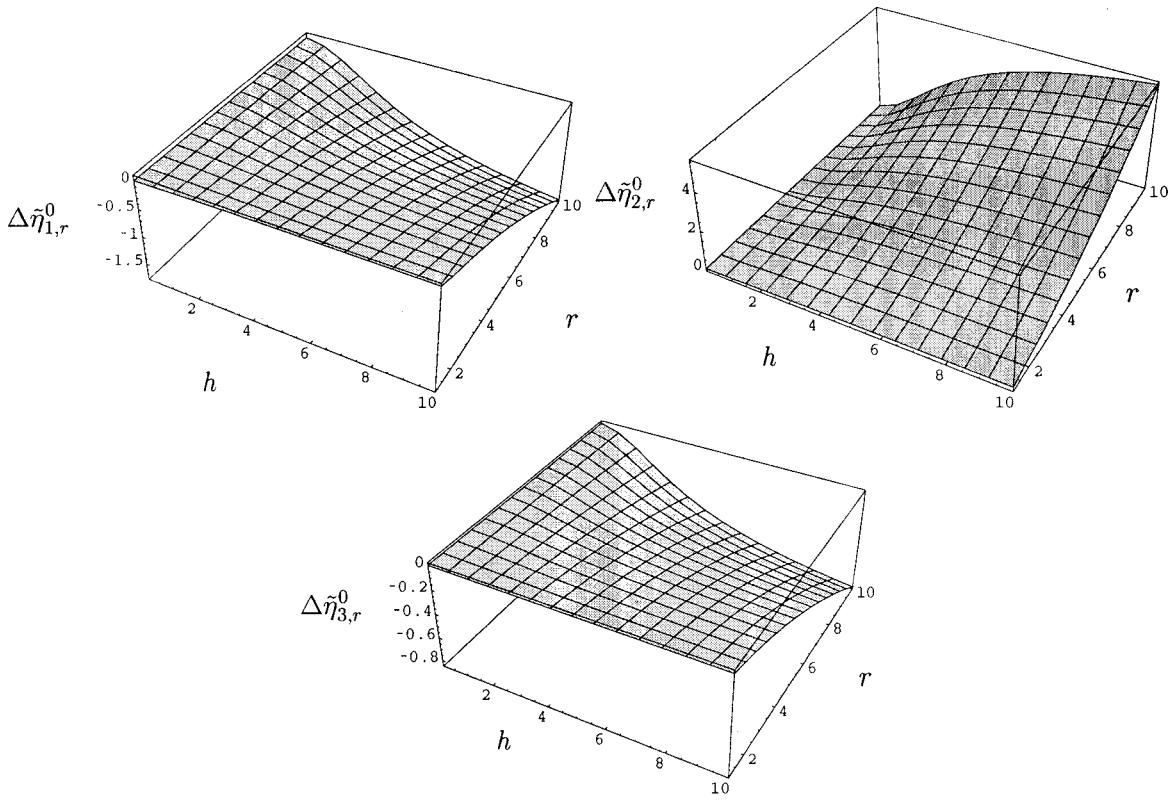

FIG. 2. Reduced Miesowicz viscosity coefficients $\Delta\tilde{\eta}^0_{i,r}\equiv(\eta^0_{i,r}-\eta_{0,r})/2\eta^\phi_0$, as a function of the reduced magnetic field h and the axis ratio r of the ellipsoid. The figures for $i=1,2,3$ from top to bottom, correspond to Eqs. (51), (52), (53) with the replacement $S_i\to S_i^{\rm eq}(h)$. We observe that $\Delta\tilde{\eta}^0_2$ is positive over the entire interval of h and r values shown and increases monotonically with increasing h and r. On the contrary, $\Delta\tilde{\eta}^0_3$ is negative and decreases monotonically with increasing h and r. Finally, $\Delta\tilde{\eta}^0_1$ is negative and decreases monotonically with increasing h and r only for large values of h and r.

tained by minimizing the free energy functional subject to fixed constraints [26,27,29],

$$F[f]\to\min,\quad \langle 1\rangle=1,\quad \langle \boldsymbol{u}\rangle=\boldsymbol{A}. \tag{65}$$

Carrying out the minimization of the functional (12) subject to the constraints (65), one obtains

$$f^*(\boldsymbol{u})=f_{\rm eq}(\boldsymbol{u})\exp(\tilde{\boldsymbol{\Lambda}}\cdot\boldsymbol{u}+\tilde{\Lambda}_0) \tag{66}$$

with the dimensionless Lagrange multipliers $\tilde{\boldsymbol{\Lambda}}$ and $\tilde{\Lambda}_0$. Averages of functions $A(\boldsymbol{u})$ with respect to the distribution function (66) are denoted by

$$\langle A\rangle_*\equiv\int d^2u A(\boldsymbol{u})f_{\rm eq}(\boldsymbol{u})\exp(\tilde{\boldsymbol{\Lambda}}\cdot\boldsymbol{u}+\tilde{\Lambda}_0). \tag{67}$$

The Lagrange multipliers $\tilde{\boldsymbol{\Lambda}}$ and $\tilde{\Lambda}_0$ are determined by the constraints

$$\langle 1\rangle_*=1,\quad \langle \boldsymbol{u}\rangle_*=\boldsymbol{A}. \tag{68}$$

Upon reparametrization, $\boldsymbol{\xi}_e=\boldsymbol{h}+\tilde{\boldsymbol{\Lambda}}$, the generalized canonical distribution (66) becomes

$$f^*(\boldsymbol{u})=\frac{\xi_e}{4\pi\sinh(\xi_e)}\exp(\boldsymbol{\xi}_e\cdot\boldsymbol{u}) \tag{69}$$

with the norm ξ_e of $\boldsymbol{\xi}_e$. Note, that the distribution functions (69) are uniaxially symmetric, $f^*(\boldsymbol{u})=f^*(\boldsymbol{u}\cdot\boldsymbol{n})$, where the director $\boldsymbol{n}$ is parallel to $\boldsymbol{\xi}_e$ and $\boldsymbol{M}^*$, $\boldsymbol{n}=\boldsymbol{\xi}_e/\xi_e=\boldsymbol{M}^*/M^*$. Therefore, results of Sec. III are also valid in the present approximation.

Comparing Eqs. (69) and (10), we observe that the QEA distribution function can be obtained from the equilibrium distribution upon replacing the magnetic field $\boldsymbol{h}$ by the so-called effective field $\boldsymbol{\xi}_e=\boldsymbol{h}+\tilde{\boldsymbol{\Lambda}}$. Thus, the so-called effective field approximation introduced in Ref. [4] is just the QEA for the special choice (65) of macroscopic variables. While this approximation gives accurate results in case of spherical particles, $B=0$ (see, e.g., [30]), the accuracy of the approximation (72) for $B\neq 0$ remains to be studied.

Moments of f^* of order four or less are given by Eqs. (E1)–(E4), where the scalar orientational order parameters S_j are now given as explicit functions of ξ_e,

$$S_j^*=L_j(\xi_e), \tag{70}$$

where functions $L_i(x)$ are defined by Eq. (22). The macroscopic magnetization $\boldsymbol{M}=n\mu\langle\boldsymbol{u}\rangle$ is obtained in terms of $\boldsymbol{\xi}_e$ as

$$\boldsymbol{M}^*=n\mu\boldsymbol{A}=n\mu L(\xi_e)\boldsymbol{\xi}_e/\xi_e. \tag{71}$$

The time evolution of the macroscopic variables $\boldsymbol{A}$, i.e., of the magnetization $\langle \boldsymbol{u} \rangle$ within the QEA, is found from Eqs. (69),(16) with the help of Eqs. (23),(70) and reads

$$\dot{\boldsymbol{A}} = \boldsymbol{\Omega} \times \boldsymbol{A} + B(\boldsymbol{D} \cdot \boldsymbol{A} - \langle \boldsymbol{uuu} \rangle_* : \boldsymbol{D}) - \frac{1}{2\tau}(\mathbf{1} - \langle \boldsymbol{uu} \rangle_*) \cdot \tilde{\boldsymbol{\Lambda}}. \tag{72}$$

The macroscopic free energy $F^*(\boldsymbol{A})$ is defined as the free energy functional (12), evaluated with the distribution function (66), $F^*(\boldsymbol{A}) = F[f^*]$. The Lagrange parameters $\tilde{\boldsymbol{\Lambda}}$ have a nice interpretation as the variables conjugate to the macroscopic ones,

$$\tilde{\boldsymbol{\Lambda}} = \frac{\partial F^*(\boldsymbol{A})}{\partial \boldsymbol{A}}. \tag{73}$$

The time rate of change of the macroscopic free energy is $\dot{F}^* = \tilde{\boldsymbol{\Lambda}} \cdot \dot{\boldsymbol{A}}$ and becomes, upon inserting Eqs. (73) and (72),

$$\dot{F} = \tilde{\boldsymbol{\Lambda}} \cdot (\boldsymbol{\Omega} \times \boldsymbol{A}) + B \tilde{\boldsymbol{\Lambda}} \cdot (\boldsymbol{D} \cdot \boldsymbol{A} - \langle \boldsymbol{uuu} \rangle_* : \boldsymbol{D}) - \frac{1}{2\tau} \tilde{\boldsymbol{\Lambda}} \cdot (\mathbf{1} - \langle \boldsymbol{uu} \rangle_*) \cdot \tilde{\boldsymbol{\Lambda}}. \tag{74}$$

Note that Eq. (74) coincides with the exact expression Eq. (14) if the latter is evaluated with f^*. This result illustrates the fact that the QEA conserves the type of dynamics, i.e., the function $F^*(\boldsymbol{A}) = F[f^*]$ is an H function of the QEA dynamics if the functional F is an H function of the underlying dynamics, while F^* is conserved by the QEA dynamics if F is conserved by the underlying dynamics [31].

A. Magnetization equation

Inserting the explicit form of the moments of order two and three into Eq. (72) and using Eq. (71) yields a closed equation for the macroscopic magnetization,

$$\dot{\boldsymbol{M}} - \boldsymbol{\Omega} \times \boldsymbol{M} = -\frac{1}{2\tau}(\tilde{\tau}_1 \mathbf{1} + \tilde{\tau}_2 \boldsymbol{MM}) \cdot \boldsymbol{\Lambda} + \lambda_2 \boldsymbol{D} \cdot \boldsymbol{M} + \lambda_3 (\boldsymbol{D} : \boldsymbol{MM}) \boldsymbol{M}, \tag{75}$$

where the dimensional Lagrange multipliers $\boldsymbol{\Lambda}$ have been introduced, $\tilde{\boldsymbol{\Lambda}} = \mu \boldsymbol{\Lambda}/(k_B T)$, and $\chi_0 = n\mu^2/(3k_B T)$ is the initial susceptibility. The coefficients $\tilde{\tau}_i, \lambda_i$ are defined as

$$\tilde{\tau}_1 = 3\chi_0 - \frac{M}{H_e}, \quad \tilde{\tau}_2 = \frac{3}{2M^2}\left[\frac{M}{H_e} - \chi_0\right], \tag{76}$$

$$\lambda_2 = \lambda_t, \quad \lambda_3 = -\frac{1}{(n\mu)^2}\frac{BS_3}{S_1^3}, \tag{77}$$

where λ_t is given by Eq. (31), M denotes the norm of the magnetization $\boldsymbol{M}$, and H_e is the norm of the dimensional effective field $\boldsymbol{H}_e = \boldsymbol{H} + \boldsymbol{\Lambda}$. Since we consider here only incompressible flows, terms proportional to trace $\boldsymbol{D}$ are absent. Equation (75) is, on the one hand, a generalization of Eq. (2.15) of Ref. [9] which does not consider terms proportional to the symmetric velocity gradient $\boldsymbol{D}$. On the other hand, Eq. (75) is a special case of Eq. (15) of Ref. [10] which contains additional terms proportional to $\boldsymbol{M} \times \boldsymbol{h}$ and $\boldsymbol{M} \times \boldsymbol{D} \cdot \boldsymbol{M}$ that cannot be derived within the present kinetic model when using the QEA. It should be mentioned that Eq. (75) is derived from the kinetic model (1), while the magnetization equations proposed in Refs. [9,10] are derived within a thermodynamic framework. Note, that in the present case, the Lagrange multipliers $\boldsymbol{\Lambda}$ are the conjugate variables to the macroscopic magnetization with respect to the free energy, Eq. (73), and play the role of the conjugate variables with respect to the energy density introduced in Ref. [10]. Note also the limitation to uniaxial symmetry. In the case of spherical particles, $B = 0$, the result of Martsenyuk *et al.* [4] is recovered from Eqs. (75), (76), and (77).

Coefficient λ_2 has been determined experimentally very recently in Ref. [11]. For an ester based commercial ferrofluid with volume fraction $\phi \approx 0.07$, a value $\lambda_2 = 0.2 \pm 0.05$ was measured, roughly independent of the strength of the magnetic field between 5 and 16 kA/m. Interpreting this result within the present kinetic model we first notice that the experiments in Ref. [11] were performed in the low Péclet number regime, Pé $\ll 1$. Thus the order parameters S_i are well approximated by their equilibrium values S_i^{eq}. Inserting Eqs. (39) and (40) into Eq. (77) we find

$$\lambda_2 \approx \lambda_2^0 \equiv -\frac{\gamma_2^0}{\gamma_1^0} = B\frac{(6+h^2)L(h) - 2h}{h^2 L(h)}. \tag{78}$$

For weak magnetic fields, like the ones employed in the experiment of Ref. [11], $\lambda_2^0 = \frac{3}{5}B + O(h^2)$ is obtained from Eq. (78). The absence of a linear term in h might explain the constant value of λ_2 observed over the interval of magnetic field strengths $5 \leqslant H\,[\mathrm{kA/m}] \leqslant 16$, approximately corresponding to $0.3 \leqslant h \leqslant 0.96$. Within the present kinetic model, the experimentally determined value $\lambda_2 = 0.2 \pm 0.05$ corresponds to an asphericity of the particles of $r = 1.4 \pm 0.1$. This value is smaller than the estimate in Ref. [11], $r = 2$, which is based on the stationary distribution (11) of ellipsoidal ferromagnetic particles in a potential flow.

As noted also in Ref. [10], the application of Eq. (75) is limited to the uniaxial regime. In general, corrections to Eq. (75) are expected in case of biaxial symmetry of the orientational distribution function for the magnetic units. For a discussion of biaxial symmetry in the case of spherical particles, see Ref. [19].

B. Stress tensor

In Ref. [10], also an expression for the symmetric stress tensor $\boldsymbol{T}^{\mathrm{s}}$ was given in terms of the conjugate variables. As shown in Sec. III, $\boldsymbol{T}^{\mathrm{s}}$ derived from the kinetic model under the assumption of uniaxial symmetry is of the Ericksen-Leslie form (A4). The comparison of this result to the stress tensor given by Eq. (16) in Ref. [10] is facilitated by rewriting the stress tensor (6) in terms of the dual variables $\boldsymbol{\Lambda}$. Within the QEA, the potential contribution to the symmetric stress tensor, $\boldsymbol{T}^{\mathrm{pot}}$, can be rewritten as

$$\boldsymbol{T}^{\mathrm{pot}}=\langle \boldsymbol{u}\rangle_{*}\tilde{\boldsymbol{\Lambda}}+\tilde{\boldsymbol{\Lambda}}\langle \boldsymbol{u}\rangle_{*}-2\langle \boldsymbol{uuu}\rangle_{*}\cdot\tilde{\boldsymbol{\Lambda}}. \tag{79}$$

Inserting the form of the moments and using the expression for the macroscopic magnetization, we find

$$\boldsymbol{T}^{\mathrm{pot}}=\frac{1}{2}\lambda_2(\boldsymbol{M\Lambda}+\boldsymbol{\Lambda M})+\lambda_3\boldsymbol{MMM}\cdot\boldsymbol{\Lambda}. \tag{80}$$

In Eq. (80), we have dropped diagonal contributions to $\boldsymbol{T}^{\mathrm{pot}}$ since we consider here only incompressible flows. Equation (80) is a special case of equation (16) in Ref. [10]. Viscous contributions to the symmetric stress tensor are, however, absent from Eq. (16) in Ref. [10] while they do occur in the kinetic model considered here, Eq. (6).

V. BROWNIAN DYNAMICS SIMULATIONS

In order to discuss the validity of several assumptions made in the previous sections, we here present simulation results of the numerical solution of the full kinetic model (1). The numerical solution to the kinetic equation (1) is obtained by Brownian dynamics (BD) simulations of the stochastic process $\boldsymbol{U}_t$ that satisfies the following stochastic differential equation corresponding to the kinetic equation [32]:

$$d\boldsymbol{U}_t=\boldsymbol{P}_t\cdot[(\boldsymbol{\Omega}\times\boldsymbol{U}_t+B\boldsymbol{D}\cdot\boldsymbol{U}_t+\boldsymbol{h})dt+d\boldsymbol{W}_t]-\boldsymbol{U}_t\frac{dt}{\tau}. \tag{81}$$

The projector perpendicular to $\boldsymbol{U}_t$ is denoted by $\boldsymbol{P}_t\equiv(\mathbf{1}-\boldsymbol{U}_t\boldsymbol{U}_t)$ and $\boldsymbol{W}_t$ is a three-dimensional Wiener process [32]. Using Itô's formula, it is verified that Eq. (81) conserves the normalization of $\boldsymbol{U}_t$. We recall that $\tau\boldsymbol{\Omega}=\mathrm{Pé}\tilde{\boldsymbol{\Omega}}$ (same for $\boldsymbol{D}$) with dimensionless tensors $\tilde{\boldsymbol{\Omega}},\tilde{\boldsymbol{D}}$ characterizing the flow geometries. The dimensionless simulation parameters are the Langevin parameter $h=\mu H/k_{\mathrm{B}}T$, the axis ratio r, and the Péclet number Pé. Dimensionless times are expressed in units of a relaxation time τ. These parameters carry information about the implicit system parameter N, cf. Sec. I. For example, for cylindrical units made of a given number N of particles, $r=N$, $h=Nh_1$, $\tau=Ne_N\tau_1$, and $\mathrm{Pé}=Ne_N\mathrm{Pé}_1$ in terms of ''microscopic'' quantities. The latter may be considered as fixed system parameters, if one is interested in the influence of chain length on the material properties. On the other hand, N and also r may be eliminated by using a further model for the effect of h and Pé on these parameters.

In order to integrate Eq. (81) numerically, a weak first-order scheme is used. By construction, the numerical scheme guarantees the normalization of the random unit vector $\boldsymbol{U}_t$ [32]. For various initial conditions, the simulations are performed for an ensemble of 10^5 random unit vectors $\boldsymbol{U}_t$ with time step $10^{-3}\tau$. Figure 3 shows the result of BD simulations for the (ensemble averaged) relaxational dynamics of the orientational order parameters S_i for a perfectly oriented initial state in a plane Couette flow with $\mathrm{Pé}=0.1$ and the magnetic field $h=1$ in the gradient direction. The value of S_1 and the director $\boldsymbol{n}$ are obtained from Eq. (E1), while the values S_i for $i>1$ are obtained assuming relations (E2)–(E4). A stationary state is attained for times $t\gtrsim 2\tau$.

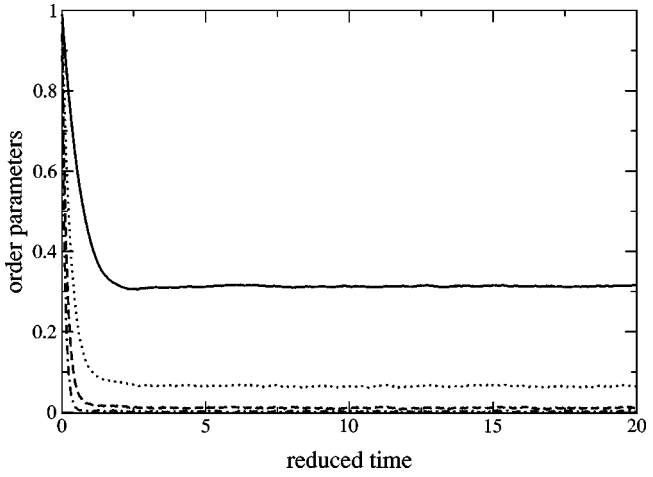

FIG. 3. Relaxational dynamics of the orientational order parameters S_i as a function of dimensionless time t/τ for a perfectly oriented initial state in plane Couette flow with $\mathrm{Pé}=0.1$ and magnetic field $h=1.0$ oriented in the gradient direction. From top to bottom the rank of the order parameters S_i increases as $i=1,2,3,4$. The order parameters are extracted from the BD simulation with the help of Eqs. (E1)–(E4). The director $\boldsymbol{n}$ and S_1 are defined by Eq. (E1), while S_2, S_3, and S_4 are determined from $\langle \boldsymbol{uu}\rangle$, $\langle \boldsymbol{uuu}\rangle$, and $\langle \boldsymbol{uuuu}\rangle$, respectively, assuming relations (E2)–(E4).

In the sequel, simulation results for the stationary state will be presented that are collected as averages over the ensemble and subsequent time averages for times $10\tau<t<20\tau$. Plane Couette flow is considered in order to allow comparison to analytical results in Sec. III C. Figures 4 and 5 show the result of the BD simulation for the reduced shear viscosities η_{a}, η_{b}, and η_{c}, for Péclet number $\mathrm{Pé}=0.1$ if the magnetic field (and not necessarily the magnetization) is oriented in the flow, gradient, and vorticity direction, respectively. Figure 4 shows the results of the BD simulations for the shear viscosities in comparison to the results in Sec. III based on the assumption of uniaxial symmetry, where the values of the director components and the order parameters were extracted from the BD simulation. It is seen from Fig. 4 that the results of Sec. III agree qualitatively with the numerical simulations and that Eqs. (26)–(29) provide a very good description of the numerical results, while Eqs. (42)–(45) do so only for strong magnetic fields. As will be seen later, the assumption of uniaxial symmetry is violated for weak magnetic fields so that results of Sec. III represent approximations to the actual viscosities. Since Eqs. (26)–(29) provide a better approximation also for this regime, we no longer consider Eqs. (42)–(45) in the sequel. For weak magnetic field, the viscosity increases quadratically, while for strong field it approaches a limiting value. Since the Péclet number is small, it is expected that the viscosity coefficients are well approximated by the Miesowicz viscosities, $\eta_{\mathrm{a}}\approx\eta_{1,r}$, $\eta_{\mathrm{b}}\approx\eta_{2,r}$, $\eta_{\mathrm{c}}\approx\eta_{3,r}$. Figure 5 shows that the agreement with the analytical predictions (51)–(53) is very good.

It should be mentioned that three different shear viscosity coefficients, η_{a}, η_{b}, and η_{c}, have indeed been observed experimentally on colloidal solutions of magnetite in tetrade-

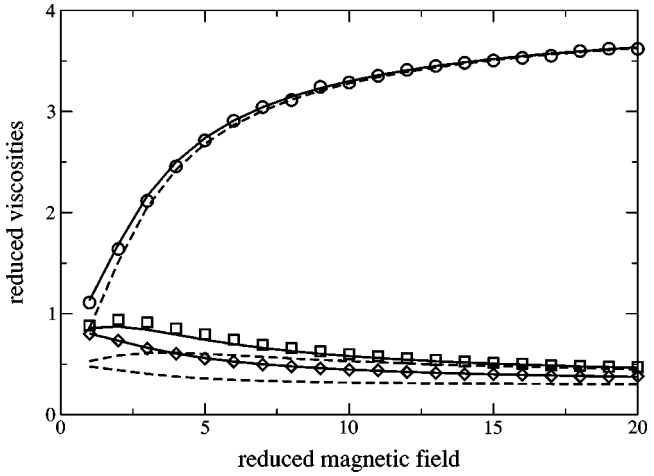

FIG. 4. Viscosity change $T_{yx}/\dot{\gamma}-\eta_s$ as a function of reduced magnetic field h for plane Couette flow $\boldsymbol{v}=(\dot{\gamma}y,0,0)$. The Péclet number is Pé$=0.1$ and the axis ratio was chosen $r=5$. The ordering of the curves from top to bottom corresponds to magnetic fields parallel to the velocity gradient, the velocity, and the vorticity direction, respectively. Symbols denote results from BD simulation, the solid and dashed lines represent the semianalytical results of Eqs. (26)–(29) and (42)–(45), respectively, where the values for the order parameters and director components were obtained from the BD simulation.

cane [33]. The authors of Ref. [33] speculate that their results might be explained by the presence of anisotropic, ellipsoidal particles and estimate their aspect ratio r. Figure 6 shows their result for the shear viscosities η_a, η_b, and η_c. The values of the magnetic field are transformed into the reduced magnetic field h assuming a temperature of $T=300$ K. According to Ref. [33], the suspension shows hydrodynamic

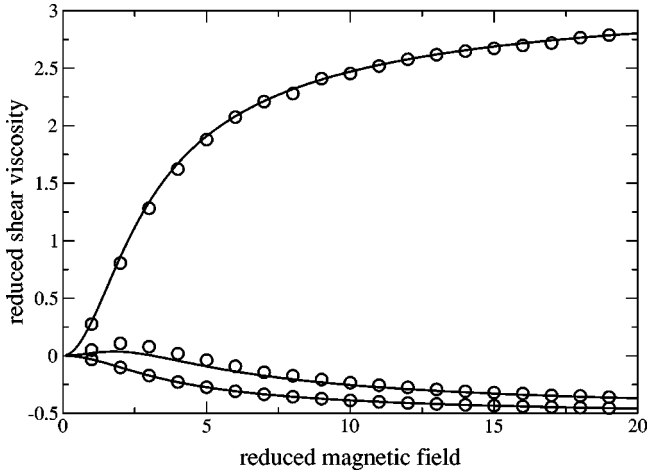

FIG. 5. Viscosity change $\Delta\tilde{\eta}^0_{i,r}$ as a function of reduced magnetic field h for plane Couette flow. The Péclet number is Pé$=0.1$ and the axis ratio was chosen $r=5$. The ordering of the curves from top to bottom is $i=2,1,3$, corresponding to magnetic fields parallel to the velocity gradient, the velocity, and the vorticity direction, respectively. Symbols denote results from BD simulation, the straight lines represent the analytical results, Eqs. (51), (52), and (53) with the replacement $S_i\rightarrow S_i^{eq}(h)$.

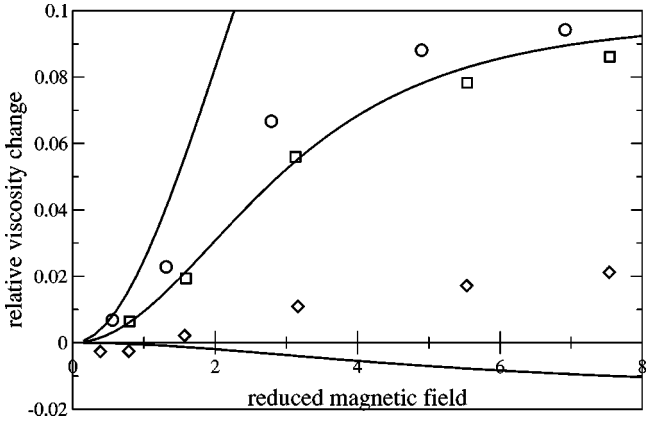

FIG. 6. Relative viscosity change R_i, Eq. (60), as a function of reduced magnetic field h for a colloidal suspension of magnetite in tetradecane. Data are taken from Ref. [33]. Also shown is a fit to the data by Eqs. (51)–(53), where the axis ratio was chosen $r=1.5$. The ordering of the curves from top to bottom is $i=2,1,3$, corresponding to magnetic fields parallel to the velocity gradient, the velocity and the vorticity direction, respectively. Symbols denote experimental results, the straight lines represent the analytical results, Eqs. (51), (52), and (53) with the replacement $S_i\rightarrow S_i^{eq}(h)$.

volume fraction of $\phi\approx 0.062$ and mean magnetic moment $\mu_1\approx 3.53\times 10^4\mu_B$ of colloidal particles. Although not stated explicitly in Ref. [33], we assume the experimental results shown in Fig. 6 were obtained in the low Péclet number regime. Thus, the relative change of shear viscosity is given by R_i^0, Eq. (60). In qualitative agreement with the present results, it is found that $\eta_b>\eta_a>\eta_c$ and $\eta_b>\eta_a>0>\eta_c$ for weak magnetic fields. However, their result $\eta_c>0$ for strong magnetic fields is not predicted by the present model. This discrepancy is most likely interpreted as a signature of the formation of structure induced by the external magnetic field, whose amount (effect on r in our notation) should depend on the applied magnetic field $\boldsymbol{h}$. In Fig. 6 also the analytical results (51)–(53) with equilibrium values for the order parameters are shown. The axis ratio r was chosen as $r=1.5$, close to the estimate $r=1.3$ of Ref. [33]. The effective magnetic moment is $\mu=r\mu_1$ since the ellipsoidal particles are considered as agglomerates of individual particles, each with individual magnetic moment μ_1. From Fig. 6 it is seen that quantitative agreement with the theoretical predictions is poor, except for η_1. In view of the qualitative difference in the behavior of $\eta_{3,r}$, we have not attempted to improve the comparison by a different fit (r is the only fit parameter in Fig. 6), by considering polydispersity effects, or the effect of the magnetic field on the shape r. In Ref. [33], also results for a different suspension showing higher anisotropy of the viscosity coefficients are shown. Since in that case neither volume fraction nor mean magnetic moment are given, no comparison to the theoretical result is shown.

In Fig. 7, the effect of the Péclet number on the shear viscosity η_2 is shown for fixed values of the magnetic field. Shear-thinning behavior is observed, in qualitative agreement with experimental results [5]. Note that an additional mechanism of shear thinning is present in ferrofluids due to the breakup of agglomerates in shear which is not included

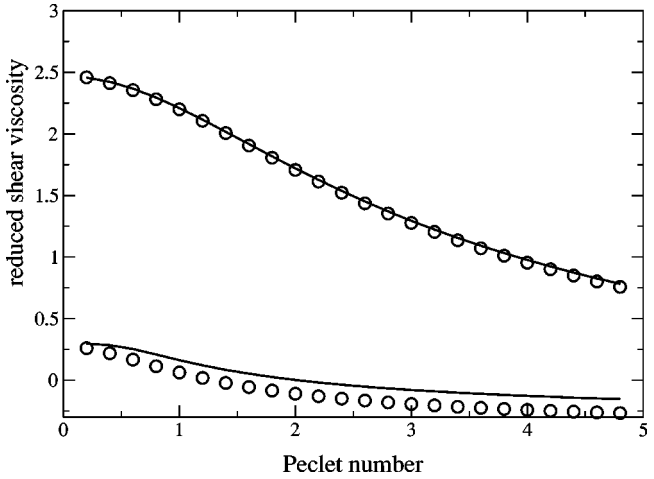

FIG. 7. Viscosity change $(\eta_b-\eta_{0,r})/2\eta_0^\phi$ as a function of Pé for plane Couette flow. The magnetic field is oriented in the gradient direction. The value of the magnetic field is $h=10$ and $h=1$ for the upper and lower curves, respectively. Symbols correspond to BD simulations, while solid lines represent the semianalytical result, Eqs. (26)–(29), where the values of the order parameters and components of the director are extracted from the BD simulation.

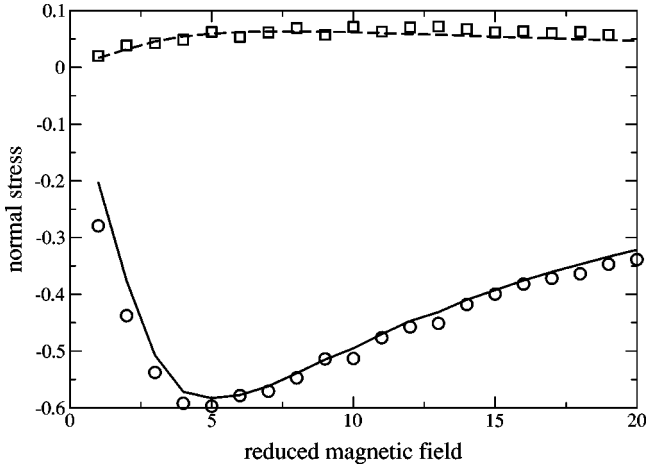

FIG. 8. Normal stress differences $N_i/2\eta_0^\phi$, with $i=1,2$, as a function of reduced magnetic field h for plane Couette flow. The magnetic field is oriented in the gradient direction. The Péclet number is Pé$=0.5$ and the axis ratio was chosen as $r=5$. Symbols indicate results of Brownian dynamics simulation (circles: $i=1$; squares: $i=2$), while solid ($i=1$) and broken ($i=2$) lines correspond to the result of the uniaxial approximation.

in the present model. For strong magnetic fields, $h\gtrsim 10$, the simulation results are well described by Eqs. (26)–(29) if the values of the order parameters and director components are extracted from the BD simulation. For weak magnetic fields, $h\lesssim 1$, we observe that the shear viscosity η_b becomes lower than the zero-shear value, $\eta_b<\eta_{0,r}$. This so-called ''negative viscosity'' effect [1] has so far been observed only in oscillating magnetic fields, while the present model predicts this effect also for sufficiently high shear rates, Pé>1, and weak magnetic fields, $h<1$. Note that it is difficult to fulfill the condition Pé>1 experimentally since most ferrofluids show relaxation times of the order of 10^{-4} s [1]. However, using high-viscosity carrier fluids, relaxation times of the order of 10 ms can be achieved (see, e.g., Ref. [34]), so that shear rates of the order of 100 s^{-1} would be sufficient to satisfy Pé>1. For weak magnetic fields, the agreement is not as good as for strong magnetic fields and becomes worse for increasing Pé. In this regime, it is expected that the assumption of uniaxial symmetry does not hold. For the highest Péclet number simulated, Pé$=10$, the results from Eqs. (26)–(29) for $h=1$ disagree with simulation results by a factor of 2.

Figure 8 shows Brownian dynamics results of the first and second normal stress coefficient N_1, N_2 as a function of h for the same flow situation with Pé$=0.5$. We observe that N_1 is negative, with a minimum value roughly around $h\approx 5$. The second normal stress coefficient N_2 is found to be positive, $N_2\ll|N_1|$, and only weakly dependent on the magnetic field h. Also shown are the semianalytical results for the case of uniaxial symmetry, calculated from Eqs. (A4) and (26)–(29) with the values S_i taken from the Brownian dynamics simulation. We observe from Fig. 8 that the agreement between these results is satisfactory and improves for increasing h.

In order to further discuss the validity of the assumption of uniaxial symmetry made in Sec. III, we define the director $\boldsymbol{n}$ by $\langle \boldsymbol{u}\rangle = S_1\boldsymbol{n}$, Eq. (E1). In the literature, there exist several measures for deviations from uniaxial symmetry. Here, we use the biaxiality parameter b defined in Ref. [35] as a function of the scalar invariants of the alignment tensor $\langle\overline{\boldsymbol{uu}}\rangle$, i.e., $b^2=1-6I_3^2/I_2^3$ with $I_2\equiv\langle\overline{\boldsymbol{uu}}\rangle:\langle\overline{\boldsymbol{uu}}\rangle$ and $I_3\equiv(\langle\overline{\boldsymbol{uu}}\rangle\cdot\langle\overline{\boldsymbol{uu}}\rangle):\langle\overline{\boldsymbol{uu}}\rangle$. One has $b=0$ in the case of uniaxial symmetry while b reaches its maximum value $b=1$ in the case of planar biaxial symmetry. Figure 9 shows Brownian dynamics results of the biaxiality parameter b as a function of h corresponding to the same flow situation and the same Péclet number as in Fig. 8. We observe from Fig. 9 that b rapidly decreases with increasing h, thus explaining the good agreement between the analytical results based on the assumption of uniaxial symmetry and the Brownian dynamics simulation for $h\gg 1$. It is interesting to note that the agreement between Brownian dynamics simulation and analytical results for uniaxial symmetry agree fairly well even for $h\approx 1$, where deviations from uniaxial symmetry do occur, as shown in Fig. 9. A similar situation was already encountered for the special case of spherical particles, where a detailed analysis showed that biaxial corrections to the uniaxial approximation were found to be small, even if the parameter b approaches values close to one.

VI. CONCLUSION

In the present work, the relationship between the kinetic model of dilute suspensions of rigid, ellipsoidal, ferromagnetic particles and the Ericksen-Leslie theory of nematic liquid crystals is established in Sec. III. It is found that for uniaxial symmetry, the predictions of the kinetic model for the stress tensor are of the same form as in the Ericksen-Leslie theory. A complete set of viscosity coefficients is obtained as a function of the orientational order parameters. In the limit of small Péclet numbers, the viscosity coefficients

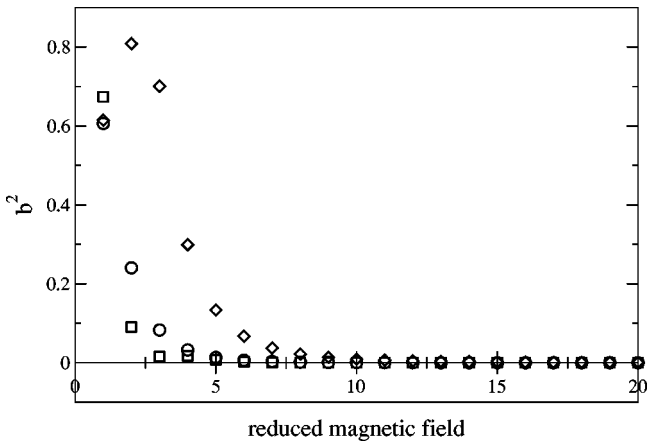

FIG. 9. Biaxiality parameter b, defined in Sec. V, as a function of reduced magnetic field h for plane Couette flow with Pé$=1.0$. Circles, squares, and diamonds correspond to the magnetic field being oriented in gradient, flow, and vorticity direction, respectively.

reduce to explicit functions of the magnetic field. For the special case of plane Couette flow, the Miesowicz viscosity coefficients, the alignment angle, and the normal stress coefficients are obtained in Sec. III C.

Predictions of the kinetic model are compared in Sec. IV to the form of the magnetization and stress equation derived within a thermodynamic framework in Ref. [10]. Within the so-called effective field approximation, the magnetization equation derived from the present kinetic model is a special case of the previous result, while the stress tensor obtained from the kinetic model generalizes the expression given in Ref. [10] due to viscous contributions. Recent experimental results [11] for the coefficient λ_2 occurring in the magnetization equation are interpreted within the present kinetic model.

Brownian dynamics simulation of the full kinetic model in plane Couette flow were performed in order to discuss the validity of the assumption of uniaxial symmetry, and thus the assumption made to proceed with the effective field approximation. It is found that the viscosity coefficients are in good agreement with the results of the uniaxial approximation, cf. Eqs. (26)–(29), (30). The agreement is enhanced for strong magnetic field, resp. low Mason numbers $\mathrm{Mn} \ll 1$. We stress that this agreement does not imply the actual distribution function to be almost uniaxially symmetric. Indeed, even for large values of the biaxiality parameter, indicating strong deviations from uniaxial symmetry, the moments that are relevant for the stress tensor are still rather well approximated by the uniaxial expressions.

The derivation of the viscosity coefficients within the uniaxial assumption is not unique. We provide also a second, nonequivalent set of viscosity coefficients that satisfy Parodi's relation. Only in the limit of strong magnetic fields do these sets of viscosity coefficients coincide. The Brownian dynamics results reveal that the agreement is better for the first set of viscosity coefficients [Eqs. (26)–(29), (30)] than the second [Eqs. (42)–(45), (30)], that satisfies Parodi's relation. Thus, violations of uniaxial symmetry by the kinetic model seem to be better approximated if the assumption of uniaxial symmetry is imposed on the form (18) of the symmetric stress tensor than on the definition (6).

Polydispersity effects and dependence of the size of the agglomerates on the magnetic field should be taken into account for improved comparison with experimental results on ferrofluids. We mention that the present approach can easily be extended to include a field-dependent size of particles $r = r(h)$ and polydispersity effects by subsequent averaging of the present results over values of axis ratios r. Following the approach of Ref. [15], the stress tensor in the uniaxial phase is still given by Eqs. (A1), where the Leslie coefficients α_i given by Eqs. (26)–(29) are replaced by their average values $\overline{\alpha_i}$. The averages are performed over all integer values of axis ratios, reflecting the assumption of cylindrical aggregates of identical spherical particles [15].

ACKNOWLEDGMENTS

The authors are thankful to S. Odenbach for providing Ref. [11] prior to publication. Financial support provided by the Deutsche Forschungsgemeinschaft (DFG) via the priority program 1104 ''Colloidal magnetic fluids'' is gratefully acknowledged. This research was supported in part by the National Science Foundation under Grant No. PHY99-07949.

APPENDIX A: DIRECTOR THEORY

We here summarize the basic equations of the Ericksen-Leslie continuum theory of anisotropic incompressible fluids with variable internal degree of alignment. The basic assumptions of the classical Ericksen-Leslie theory of nematic liquid crystals [18,23] are that the internal structure is described by a unit vector field $\boldsymbol{n}(\boldsymbol{x};t)$ (called the director) and that the stress tensor $\boldsymbol{T}$ is a linear function of the symmetric velocity gradient $2\boldsymbol{D} \equiv \boldsymbol{\nabla v} + (\boldsymbol{\nabla v})^T$ and the corotational derivative of $\boldsymbol{n}$, $\boldsymbol{N} \equiv \dot{\boldsymbol{n}} - \boldsymbol{\Omega} \times \boldsymbol{n}$, where $2\boldsymbol{\Omega} = \boldsymbol{\nabla} \times \boldsymbol{v}$ is the vorticity of the flow,

$$\boldsymbol{T} = \alpha_1 (\boldsymbol{nn}:\boldsymbol{D})\boldsymbol{nn} + \alpha_2 \boldsymbol{nN} + \alpha_3 \boldsymbol{Nn} + \alpha_4 \boldsymbol{D} + \alpha_5 \boldsymbol{nn} \cdot \boldsymbol{D} + \alpha_6 \boldsymbol{D} \cdot \boldsymbol{nn}. \tag{A1}$$

In the absence of body forces, the balance of linear momentum reads

$$\rho \dot{\boldsymbol{v}} = -\boldsymbol{\nabla} p + \boldsymbol{\nabla} \cdot \boldsymbol{T}^T, \tag{A2}$$

where ρ denotes the density of the fluid and p the pressure. Neglecting director inertia and surface stresses, the director $\boldsymbol{n}$ obeys the balance equation

$$\boldsymbol{0} = (\boldsymbol{1} - \boldsymbol{nn}) \cdot [\boldsymbol{h_n} - \gamma_1 \boldsymbol{N} - \gamma_2 \boldsymbol{D} \cdot \boldsymbol{n}], \tag{A3}$$

where $\boldsymbol{h_n}$ is the external director body force.

It is useful to decompose the stress tensor $\boldsymbol{T}$ into its symmetric and antisymmetric part, $\boldsymbol{T} = \boldsymbol{T}^{\mathrm{s}} + \boldsymbol{T}^{\mathrm{a}}$, where

$$\boldsymbol{T}^{\mathrm{s}}=\alpha_1(\boldsymbol{nn}:\boldsymbol{D})\boldsymbol{nn}+\frac{1}{2}(\alpha_2+\alpha_3)(\boldsymbol{nN}+\boldsymbol{Nn})+\alpha_4\boldsymbol{D}+\frac{1}{2}(\alpha_5+\alpha_6)(\boldsymbol{D}\cdot\boldsymbol{nn}+\boldsymbol{nn}\cdot\boldsymbol{D}), \tag{A4}$$

$$\boldsymbol{T}^{\mathrm{a}}=-\frac{1}{2}\gamma_1(\boldsymbol{nN}-\boldsymbol{Nn})-\frac{1}{2}\gamma_2(\boldsymbol{nn}\cdot\boldsymbol{D}-\boldsymbol{D}\cdot\boldsymbol{nn}).$$

The viscosity coefficients α_i are commonly known as Leslie coefficients. The coefficients γ_i are related to α_i by

$$\gamma_1=\alpha_3-\alpha_2,$$

$$\gamma_2=\alpha_6-\alpha_5. \tag{A5}$$

In the Ericksen-Leslie theory, the six viscosity coefficients remain undetermined phenomenological parameters, restricted only by dissipation arguments [36],

$$\alpha_4\geqslant 0, \quad \gamma_1\geqslant 0, \tag{A6}$$

$$2\alpha_4+\alpha_5+\alpha_6-\gamma_2^2/\gamma_1\geqslant 0. \tag{A7}$$

APPENDIX B: ROTARY FRICTION COEFFICIENT

The exact original result for the rotary friction coefficient ζ_{rot} of a single prolate ($r>1$) ellipsoid is [37]

$$\zeta_{\mathrm{rot}}=8\pi\eta_{\mathrm{s}}a^3e_r, \tag{B1}$$

with

$$e_r=\frac{2}{3}\left(1-\frac{1}{r^4}\right)\left[\frac{2r^2-1}{2r\sqrt{r^2-1}}\ln\left(\frac{r+\sqrt{r^2-1}}{r-\sqrt{r^2-1}}\right)-1\right]^{-1}. \tag{B2}$$

In terms of the geometric coefficients B and Q_0 defined below the dimensionless factor e_r that occurs due to asphericity of particles, can be expressed as

$$e_r=\frac{5}{3}\frac{Q_0}{B}. \tag{B3}$$

For slightly deformed spheres with axis ratio $r=1+\epsilon$ and $\epsilon\ll 1$, one gets

$$e_r=1-\frac{9}{5}\epsilon+\frac{1089}{350}\epsilon^2+O(\epsilon^3) \quad \text{for} \quad r=1+\epsilon, \tag{B4}$$

while the opposite limit, $r\gg 1$, gives

$$e_r=\frac{2}{3[2\ln(2r)-1]} \quad \text{for} \quad r\gg 1. \tag{B5}$$

The latter expression (B5) represents a good approximation already for $r\gtrsim 2$.

APPENDIX C: GEOMETRIC CONSTANTS

The geometric coefficients Q_i depend only on the axis ratio r of the ellipsoid and are given explicitly by [20]

$$Q_0=\frac{2(r^2-1)^2}{5r^2(2r^2\beta-\beta-1)},$$

$$Q_1=\frac{4(r^2-1)^2}{5r^2(3\beta+2r^2-5)},$$

$$Q_2=\frac{2Q_1}{3}\left[1-\frac{2r^2+1-(4r^2-1)\beta}{4(2r^2+1)\beta-12}\right], \tag{C1}$$

$$Q_3=Q_1\left[\frac{[r^2(\beta+1)-2](3\beta+2r^2-5)}{4[\beta(2r^2-1)-1](r^2+2-3r^2\beta)}-1\right],$$

and

$$Q_{23}\equiv 3Q_2+4Q_3, \quad Q_{32}\equiv Q_3-Q_2, \tag{C2}$$

for convenience, where

$$\beta=\frac{1}{r\sqrt{|r^2-1|}}\times\begin{cases}\cosh^{-1}r & \text{for} \quad r>1,\\ \cos^{-1}r & \text{for} \quad r<1.\end{cases} \tag{C3}$$

In Refs. [1,15], a different notation for the coefficients Q_i is used, $\beta_n=5\phi Q_0$, $\alpha_n=5\phi Q_1$, $\zeta_n=5\phi(2Q_3-BQ_0)$, $\chi_n=-5\phi(Q_{23}-2BQ_0)$, $\lambda_n=B$, and $n=r$.

In order to reobtain the results for spherical units $r=1$ from this manuscript, one just sets $e_r=1$, $B=0$, $Q_{0,2,3,23,32}=0$, and $Q_1=1/2$ [the latter is not obvious at first glance from Eq. (C1), see also Eq. (D1) for the case of slightly deformed spheres] in all equations (we omitted the appearance of Q_0/B terms therefore), or visit our foregoing work [19] as an alternative.

APPENDIX D: SLIGHTLY DEFORMED SPHERES

For slightly deformed sphere with axis ratio $r=1+\epsilon$, $\epsilon\ll 1$ one finds $B=\epsilon$ and for the geometric coefficients Q_i up to $O(\epsilon^2)$:

$$Q_0=\frac{3\epsilon}{5}-\frac{9\epsilon^2}{50}, \quad Q_1=\frac{1}{2}-\frac{\epsilon}{7}+\frac{47\epsilon^2}{294},$$

$$Q_2=-\frac{2\epsilon}{7}+\frac{\epsilon^2}{21}, \quad Q_3=\frac{3\epsilon}{14}-\frac{13\epsilon^2}{2940}. \tag{D1}$$

Consequently, the Leslie viscosity coefficients (26)–(29) are given to lowest order in ϵ as

$$\alpha_1=-2\eta_0^{\phi}\frac{92\epsilon^2}{735}S_4,$$

$$\alpha_2+\alpha_3=-4\eta_0^{\phi}\left[\frac{3\epsilon}{5}-\frac{9\epsilon^2}{50}\right]S_2, \tag{D2}$$

$$\alpha_4-2\eta_{0,r}=4\eta_0^{\phi}\left[\frac{\epsilon}{7}S_2-\epsilon^2\left(\frac{51}{3430}S_2-\frac{92}{25725}S_4\right)\right],$$

$$\alpha_5+\alpha_6=2\,\eta_0^{\phi}\left[\frac{6\epsilon}{7}S_2-\epsilon^2\left(\frac{153}{1715}S_2-\frac{368}{5145}S_4\right)\right],$$

with the zero-shear viscosity $\eta_{0,r=1+\epsilon}=\eta_s+\eta_0^{\phi}(1+52\epsilon^2/175)$. In the limit $\epsilon\to 0$, the viscosity coefficients γ_1 and γ_2 are given by Eq. (30) with $\Gamma\equiv nk_BT/D_r=\eta_0^{\phi}[12/5-18\epsilon/25]$.

APPENDIX E: MOMENTS FOR THE UNIAXIAL PHASE

Considering uniaxial symmetry of the orientational distribution function (21), its first moments are expressed in terms of a director $\boldsymbol{n}$ and scalar order parameters S_i defined in Eq. (21):

$$\langle \boldsymbol{u}\rangle = S_1\boldsymbol{n}, \tag{E1}$$

$$\langle \boldsymbol{uu}\rangle = S_2\boldsymbol{nn}+\frac{1-S_2}{3}\mathbf{1}, \tag{E2}$$

$$\langle \boldsymbol{uuu}\rangle = S_3\boldsymbol{nnn}+\frac{S_1-S_3}{5}(\mathbf{1n})_{\mathrm{sym}}, \tag{E3}$$

$$\langle \boldsymbol{uuuu}\rangle = S_4\boldsymbol{nnnn}+\frac{S_2-S_4}{7}(\mathbf{1nn})_{\mathrm{sym}} + \frac{7-10S_2+3S_4}{105}(\mathbf{11})_{\mathrm{sym}}, \tag{E4}$$

where subscript sym denotes symmetrization in all indices.

[1] E. Blums, A. Cebers, and M. M. Maiorov, *Magnetic Fluids* (de Gruyter, Berlin, 1997).
[2] S. Odenbach, Int. J. Mod. Phys. B **14**, 1615 (2000).
[3] S. Odenbach, *Magnetoviscous Effects in Ferrofluids*, Lecture Notes in Physics (Springer, Berlin, 2002).
[4] M. A. Martsenyuk, Y. L. Raikher, and M. I. Shliomis, Zh. Eksp. Teor. Fiz. **65**, 834 (1973) [Sov. Phys. JETP **38**, 413 (1974)].
[5] S. Odenbach and H. Störk, J. Magn. Magn. Mater. **183**, 188 (1998).
[6] S. Odenbach and K. Raj, Magnetohydrodynamics (N.Y.) **36**, 379 (2000).
[7] B. U. Felderhof and H. J. Kroh, J. Chem. Phys. **110**, 7403 (1990).
[8] M. Liu, Phys. Rev. Lett. **70**, 3580 (1993).
[9] B. U. Felderhof, Phys. Rev. E **62**, 3848 (2000).
[10] H. W. Müller and M. Liu, Phys. Rev. E **64**, 061405 (2001).
[11] S. Odenbach and H. W. Müller, Phys. Rev. Lett. **89**, 037202 (2002).
[12] M. A. Martsenyuk, J. Appl. Mech. Tech. Phys. **14**, 564 (1973).
[13] K. M. Jansons, J. Fluid Mech. **137**, 187 (1983).
[14] A. Cebers, Magnetohydrodynamics **20**, 349 (1984).
[15] A. Y. Zubarev and L. Y. Iskakova, Phys. Rev. E **61**, 5415 (2000).
[16] A. Y. Zubarev, JETP **93**, 80 (2001).
[17] S. Hess, Z. Naturforsch. A **31A**, 1034 (1976).
[18] F. M. Leslie, Arch. Ration. Mech. Anal. **28**, 256 (1968).
[19] P. Ilg, M. Kröger, and S. Hess, J. Chem. Phys. **116**, 9078 (2002).
[20] M. Kröger and H. S. Sellers, J. Chem. Phys. **103**, 807 (1995).
[21] H. Brenner and D. W. Condiff, J. Colloid Interface Sci. **47**, 199 (1974).
[22] C. P. Borgmeyer and S. Hess, J. Non-Equilib. Thermodyn. **20**, 359 (1995).
[23] S. Chandrasekhar, *Liquid Crystals*, 2nd ed. (Cambridge University Press, Cambridge, 1992).
[24] B. U. Felderhof, Magnetohydrodynamics **36**, 396 (2000).
[25] S. Hess, T. Weider, and M. Kröger, Magnetohydrodynamics **37**, 297 (2001).
[26] R. Balian, *From Microphysics to Macrophysics. Vol. 2: Methods and Applications of Statistical Physics*, 2nd ed. (Springer-Verlag, Berlin, 1992).
[27] A. N. Gorban, *Equilibrium Encircling (Nauka, Novosibirsk, 1984)*, Chap. 3, pp. 92–132.
[28] P. Ilg, *Reduced Description of Kinetic Models of Polymer Dynamics* (Wissenschaft & Technik Verlag, Berlin, 2002).
[29] E. T. Jaynes, in *Papers on Probability, Statistics and Statistical Physics*, edited by R. D. Rosenkranz (Reidel, Dordrecht, 1983).
[30] A. Cebers, Magnetohydrodynamics **21**, 357 (1985).
[31] A. N. Gorban, I. V. Karlin, P. Ilg, and H. C. Öttinger, J. Non-Newtonian Fluid Mech. **96**, 203 (2001).
[32] H. C. Öttinger, *Stochastic Processes in Polymeric Fluids* (Springer, Berlin, 1996).
[33] A. Grants, A. Irbitis, G. Kronkalns, and M. M. Maiorov, J. Magn. Magn. Mater. **85**, 129 (1990).
[34] F. Gazeau, C. Baravian, J.-C. Bacri, R. Perzynski, and M. I. Shliomis, Phys. Rev. E **56**, 614 (1997).
[35] P. Kaiser, W. Wiese, and S. Hess, J. Non-Equilib. Thermodyn. **17**, 153 (1992).
[36] J. L. Ericksen, Arch. Ration. Mech. Anal. **113**, 97 (1991).
[37] G. B. Jeffery, Proc. R. Soc. London, Ser. A **102**, 161 (1922).